Department of Civil and Environmental Engineering

Composition of abraded dust from asphalt pavement produced using ferrochromium smelter slag (OKTO-aggregate)

Michalina Makowska, Jussi Leveinen,
Terhi Pellinen, Riikka Marjamaa

Aalto University | SCIENCE + TECHNOLOGY | RESEARCH REPORT

Aalto University publication series
SCIENCE + **TECHNOLOGY** 1/2015

Composition of abraded dust from asphalt pavement produced using ferrochromium smelter slag (OKTO-aggregate)

Michalina Makowska, Jussi Leveinen, Terhi Pellinen, Riikka Marjamaa

Aalto University
School of Engineering
Department of Civil and Environmental Engineering
Highway Engineering

Aalto University publication series
SCIENCE + **TECHNOLOGY** 1/2015

ISBN 978-952-60-6104-7 (pdf)
ISSN-L 1799-4896
ISSN 1799-4896 (printed)
ISSN 1799-490X (pdf)
http://urn.fi/URN:ISBN:978-952-60-6104-7

Unigrafia Oy
Helsinki 2015

Finland

Author

Author(s): Michalina Makowska, Jussi Leveinen, Terhi Pellinen, Riikka Marjamaa

Name of the publication

Composition of abraded dust from asphalt pavement produced using ferrochromium smelter slag (OKTO-aggregate)

Publisher School of Engineering

Unit Department of Civil and Environmental Engineering

Series Aalto University publication series SCIENCE + TECHNOLOGY 1/2015

Field of research Highway Engineering

Abstract

This report describes an investigation that took place at Aalto University commissioned by the Finnish Transport Agency about asphalt dust containing OKTO-aggregate. In the fall of 2013, Finnish newspaper headlines began to raise the issue of the occurrence of damaged timing belts in the Oulu region. It seemed to only concern certain models and was found in the form of a dust. The press reasoned that this "mysterious" dust must have originated from the aggregates abraded from the local Oulu roads. More specifically, it was attributed to the OKTO-aggregate used in surface wearing course mixtures on high traffic volume roads.

The OKTO-aggregate (OKTO-murske in Finnish) is a brand name for the man-made byproduct of the smelter slag from the Outokumpu Tornio ferrochromium plant. Natural rock aggregates are substituted by this material in high volume roads due to its excellent abrasion resistance against studded tire wear.

The conclusion is that the possible contribution of OKTO-aggregate to the mechanical breakage or abrasion of car parts was considered insignificant compared with the other fragments, such as corundum, that were also detected in the car dust. Furthermore, OKTO-aggregate was found to be much less reactive with deicing salts than the rock aggregate used in the Oulu region. Therefore, the OKTO-aggregate does not significantly contribute to the chemical corrosion of car parts.

Keywords Asphalt, ferrochromium, smelter slag, OKTO-aggregate, road dust, timing belt damages, SEM-ESD

ISBN (printed)	**ISBN (pdf)** 978-952-60-6104-7	
ISSN-L 1799-4896	**ISSN (printed)** 1799-4896	**ISSN (pdf)** 1799-490X
Location of publisher Helsinki	**Location of printing** Helsinki	**Year** 2015
Pages 46+9	**urn** http://urn.fi/URN:ISBN:978-952-60-6104-7	

TABLE OF CONTENTS

ABBREVIATIONS

AB	Asphalt concrete (asfalttibetoni)
KaM	Crushed aggregate (kalliomurske)
FE SEM	Field Emission Scanning Electron microscope (kenttäemissio pyyhkäisy elektronimikroskooppi)
EDS	Energy dispersive spectrometry (energia dispersiivinen spektri)
FT-IR	Fourier Transform Infrared spectroscopy (infrapuna spektroskopia)
PWR (SRK)	Pavement Wear Resistance device (sivurullakulutuslaite)
PRALL	Prall wear tester (Prall testi, nastarengaskuluminen)
SMA	Stone Mastic Asphalt (kivimastiksiasfaltti)
XRD	X-Ray Diffraction (röntgen diffraktio)
XRF	X-Ray Fluoresense (röntgen fluoresenssi)

SAATESANAT

Tämä tutkimus ” *OKTO-mursketta sisältävän tiepäällysteen nastojen irrottaman aineksen ominaisuudet*" tehtiin Aalto-yliopiston Yhdyskunta- ja ympäristötekniikan laitoksen Georakentamisen tutkimustyhmässä yhteistyössä Lapin AMK:n Kemin yksikön kanssa, jossa tutkimusta johti yliopettaja Timo Kauppi. Aalto-yliopiston tutkimusryhmä koostui seuraavista henkilöistä: päätutkija tietekniikan prof. Terhi Pellinen, tutkijat rakennusgeologian professori Jussi Leveinen, tohtori-opiskelija, MSc Chemial Engineer Michalina Makowska, georakentamisen maisteriopiskelija Riikka Marjamaa ja tietekniikan laboratoriomestari Petri Peltonen. Laboratoriossa tutkitut näytteet on otettu vuoden 2013 puolella ja laboratoriokokeet on tehty kevättalvella 2014.

Lisäksi Geologisen tutkimuskeskuksen Suomen geotieteiden tutkimuslaboratorio (SGL) teki SEM-ESD analyysit tutkijoina erikoistutkija FM Bo Johansson ja vanhempi geologi FM Marja Lehtonen. SEM-EDS analyysi on skannaavalla elektronimikroskoopilla tehty energia dispersiivisen spektrin mittaamiseen perustuva koostumusanalyysi.

Tohtori-opiskelija MSc. Michalina Makowska on vastannut luvuissa 2 – 4 ja 7 esitetyistä tutkimuksista ja niiden raportoinnista ja prof. Jussi Leveinen ohjasi luvuissa 5 ja 6 esitettyjä tutkimuksia ja osallistui niiden raportointiin.

Tutkimuksen kokonaisohjauksesta ja rahoituksesta vastasi päällysteiden ylläpidon hankinnan asiantuntija DI Katri Eskola, Liikennevirastosta. Pohjois-Pohjanmaan ELY-keskus (PoP ELY) vastasi tutkittavien tiemateriaalien valinnasta ja hankinnasta.

LAAJENNETTU TIIVISTELMÄ

Syksyllä 2013 lehdistössä uutisoitiin mysteeripölystä, joka kerääntyy autojen moottoritilaan ja rikkoo autojen jakopään hammashihnoja ja hammaspyöriä Oulun alueella. Salaperäisen pölyn arveltiin olevan peräisin OKTO-murskeeksi kutsutusta Outokummun Tornion ferrokromitehtaan kuonasta, jota käytetään etenkin Oulun alueella vilkasliikenteisten maanteiden asfalttipäällysteissä sen hyvän nastarengaskulutuskestävyyden takia. Aalto-yliopisto tutki asiaa Liikenneviraston toimeksiantona yhteistyössä Lapin AMK:n kanssa ja tässä raportissa esitetään Aalto-yliopiston tulokset.

Johtopäätelmä on, että OKTO-murske ei ole syypää hammashihnojen rikkoontumiseen. Hammashihnat rikkoutunevat todennäköisesti korroosion ja moottoritilaan kertyvän ja siellä kehittyvän hankaavan pölyn yhteisvaikutuksesta. Lisäksi Lapin AMK:n erikseen tekemästä pienimuotoisesta kyselystä ilmeni, että autojen hammashihnojen ennenaikaista rikkoontumista esiintyy satunnaisesti myös muualla Suomessa ja tilastollisesti luotettavasti ei voida osoittaa, että ongelma olisi keskittynyt joihinkin automerkkeihin ja pelkästään Oulun alueelle, kuten lehdistössä oli uutisoitu.

Aalto-yliopisto tutki Oulun alueelta saamiaan näytteitä OKTO-murskeesta, asfaltista ja kiviaineksista (taulukko1). Lisäksi tutkittiin pölynäytteitä, jota oli kerätty autoista Oulun alueelta Lapin AMK:n toimesta. Tutkimuksessa käytettiin referenssinä Koskenkylän (Uusimaa) ja Teiskon (Pirkanmaa) kiviaineksia sekä tyypillistä asfaltissa täytejauheena käyteltävää kalkkifilleriä ja lentotuhkaa. OKTO-murskeen tutkimuksissa käytettiin Suomen geotieteellisen tutkimuslaboratorion (SGL) uutta elektronimikroskooppia, jolla selvitettiin OKTO-murskeen tyypillistä mineraalijakaumaa ja pitoisuuksia. Kyseinen kenttäemissio elektronimikroskooppi on varustettu myös erityisellä rakeisten materiaalien tutkimuksiin kehitetyllä analyysiohjelmistolla, jonka avulla on pystytty tunnistamaan yksittäisiä, tietyn koostumuksen omaavia mikrorakeita pölynäytteistä. Aalto-yliopiston tutkimukset täydennettynä SGL:n analyysein osoittivat autoista kerätyn pölyn sisältävän merkittäviä määriä rautakloridia, joka on syövyttävä rauta- ja kloridi-ionien muodostama ioniyhdiste; hyvin pieninä pitoisuuksina OKTO-murskeen rakeita (0,03 – 0,1%); sekä pieniä pitoisuuksia erittäin kovaa mineraalia, korundia (0,04-0,1%). Lapin AMK:ssa tehtyjen elektronimikroskooppitutkimusten tulokset olivat samansuuntaisia (Sassi 2014). Merkittävät rautakloridipitoisuudet autojen moottoritilaan kertyvästä pölyssä voidaan selittää korroosiolla. Liukkaudentorjunta-aineet syövyttävät sekä autoja että asfaltin kiviaineksia. Aiemmat tutkimukset ovat osoittaneet, että lämpötilan ja kosteuden vaikutus, eli säilytetäänkö autoa autotallissa vai ulkona, vaikuttavat merkittävästi korroosioon syntyyn ja määrään (Vestola ym. 2006). OKTO-murske ei ole syypää rautakloridin muodostumiseen tai korroosioon sillä rautakloridia muodostui laboratoriokokeissa ainoastaan luonnonkiviainesten kanssa. Korroosion tuottaman rautakloridin on muissa tutkimuksissa (Cai ym. 2007) havaittu lisäävän kumin korroosiota.

Pölynäytteissä havaittu korundi on toiseksi kovin mineraali timantin jälkeen ja on mahdollista, että jopa pienet pitoisuudet korundia kuluttavat hammaspyöriä, mikä edesauttaa metalliosien korroosiota. Korundi on luonnon mineraalina hyvin harvinainen ja sen esiintymiä tunnetaan Suomessa lähinnä Lapin kulta-alueilta. Korundi on koostumukseltaan puhdasta alumiinioksidia ja sitä tavataan luonnossa kivissä, jotka ovat piiköyhiä mutta alumiinirikkaita. Tällaiset kivet ovat ylipäätänsä harvinaisia ja Oulun seudulla tiemateriaalina käytetyt amfiboliitit eivät sellaisia ole. Synteettistä korundia käytetään erilaisissa hioma-aineissa ja –laikoissa sekä täytemateriaalina kumissa, muovissa ja erilaisissa eristemassoissa parantamaan

niiden lämmönjohtavuutta. Korundin alkuperää näytteistä ei sinällään tutkittu, se ei kuitenkaan ole peräisin OKTO-murskeesta.

Tutkimuksessa Aalto-yliopisto irrotti pölyä asfalttinäytteistä nastarengaskulutusta simuloivalla sivurullakulutuslaiteella (SRK), joka on kuvassa 3. SRK-laite on kehitetty Suomessa asfalttimassan ja kiviainesten nastakulumiskestävyyden testaamiseen menetelmän SFS-EN12697-16B mukaan. Suomessa ainoastaan Aalto-yliopistolla on toimiva SRK-laite. Toisin kuin tieltä tai auton osista kerätty pöly, joka sisältää kaikkia ilman epäpuhtauksia, SRK-laitteen avulla voidaan irrottaa tutkimuksiin pölyä, joka on peräisin vain asfalttimassasta.

SRK laitetta jouduttiin modifioimaan nastapölyn talteenottoa varten ja lisäksi menetelmän toimivuuden varmistamiseksi irrotettua materiaalia tutkittiin infarapuna spektroskopian avulla (FT-IR). Valokuva laitejärjestelystä ja sedimenttitankeista on esitetty kuvassa 4 ja kuvassa 2 on valokuva asfalttinäytteestä, jota on kulutettu SRK-laitteella.

Koska asfalttipölyn irrotusmenetelmä oli uusi ja se kehitettiin tämän tutkimuksen tarpeisiin, oli tarpeellista tutkia irrotettua pölyä menetelmän toimivuuden varmistamiseksi. FT-IR analyysi tehtiin asfalttimassasta irrotetulle pölylle ja OKTO-murskeesta jauhetulle kuonapölylle. Tutkittuja asfalttimassoja oli kahta lajia, toinen referenssinä käytettyä normaalia asfalttibetonia (AB16) ja toinen kivimastiksiasfalttia (SMA22), jossa oli käytetty OKTO-mursketta, kuvat 8 ja 9. Tulosten perusteella voitiin todeta, että kehitetty menetelmä asfalttipölyn irrottamiseksi päällysteestä oli onnistunut ja SRK-pöly sisälsi OKTO-mursketta.

Asfalttinormien 2011 mukainen asfalttimassan kulutuskestävyyden Prall-testaus osoitti, että OKTO-murskeesta tehty asfalttimassa täytti parhaan kulumisluokan Abr_{A20} vaatimuksen. Tämä varmistaa käsityksen, että OKTO-murske on eriomaisesti nastarengaskulutusta kestävää materiaalia ja siitä irtoaa vähemmän asfalttipölyä kuin tavallisesta tiepäällysteestä.

Tielaboratorioon tuodun OKTO-murskeen laatua ja edustavuutta tutkittiin XRF ja XRD laitteilla ja tuloksia verrattiin materiaalin valmistajan ilmoittamiin tietoihin. Tulokset osoittivat tyypillistä koostumusta ja havaitut erot olivat lähinnä analyysimenetelmistä, näytteenotosta ja jakamisesta johtuvia. Murskauksessa ja jauhautumisessa eri raekokofraktioihin muodostuu jonkin verran koostumusvaihtelua, mutta kromipitoisuudet olivat kuonapölyssäkin merkittäviä. Tämä tukee SRK-näytteistä saatuja FT-IR-tuloksia ja voidaan todeta, että OKTO-murske jättäisi asfaltista irtoavaan pölyyn ja hienoainekseen tunnistettavan kromisignaalin.

Elektronimikroskooppi tutkimusten tavoitteena oli selvittää voidaanko OKTO-mursketta havaita SRK-laitteella kulutetusta pölystä ja voidaanko samanlaisia havaintoja tehdä auton moottoritilasta kerätystä pölystä sekä ovatko määrä samaa suuruusluokkaa. Tutkituissa SRK-pölynäytteissä noin 39 % partikkeleista oli peräisin OKTO-murskeesta kun alkuperäisessä kiviainesseoksessa OKTO-mursketta oli 67 %. Täytejauheena käytetystä kalkkifilleristä peräisin olevaa kalsiittia ja dolomiittia oli partikkeleissa 4 % eli hieman vähemmän kuin suhteitettu 6 %. Valtaosa partikkeleista oli peräisin kiviainesseoksessa käytetystä kalliokiviaineksesta, jossa valtakivilaji on amfiboliitti, sekä aksessorisista juonikivilajeista. OKTO-murskeen suhteitusta vähäisempi määrä näytteissä osaltaan vahvistaa käsitystä, että OKTO-murskeen kulutuskestävyys on parempi kuin käytetyssä kalliokiviaineksessa.

Autojen jakohihnakoteloista kerätyissä näytteissä valtaosassa rakeista oli rautaa, ruostetta ja pölyä, joka oli peräisin tavallista kiveä muodostavista mineraaleista. OKTO-murske palasten osuus oli marginaalinen (taulukko 8). Moottoritilan pölynäytteistä tehtiin myös FE-SEM analyysin yhteydessä pistemäisiä koostumusanalyysejä energia dispersiivisellä spektrianalytiikalla. Tulokset osittivat merkittäviä kloridipitoisuuksia. Lisäksi voitiin päätellä, että kloridi oli saostunut rautakloridina. Aikaisempien tutkimusten perusteella rautakloridin tiedetään muodostuvan rautaoksidien ja rautahydroksidien kanssa. Nyt haluttiin myös selvittää, onko rautakloridi voinut syntyä tiesuolan ja kiviaineksen välisessä reaktiossa.

Korroosiota tutkittiin vertaamalla OKTO-mursketta referenssikiviin Oulun alueelta ja Etelä-Suomesta sekä tavanomaiseen tiepäällysteissä täytejauheena käytettävään kalkkifilleriin. Tulokset osoittivat päinvastaista. OKTO-murske ei reagoinut suoloihin, kun taas tavalliset murskeet olivat korroosioituvia (kuvat 14 – 16).

Koska lehdistössä oli spekulaatiota autojen jakohihnojen vaurioiden pakallisuudesta ja keskittymisestä vain Oulun alueelle, selvitettiin myös suolauksen käyttöä eri puolilla Suomea. Tulokset eivät osoittaneet, että Oulussa olisi merkittävästi muuta Suomea poikkeavaa tiesuolan käyttöä (taulukko 9). Suolauksessa käytetään pääasiassa natriumkloridia ja vähäisessä määrin kalsiumkloridia. Kidevedellistä kalsiumkloridia käytetään maanteillä lähinnä kesäkaudella pölyn sitomiseen ja talvisin vähäisessä määrin yhdessä natriumkloridin kanssa valtateiden tienpintojen sulana pitämiseen. Kalsiumkloridin on todettu aiheuttavan natriumkloridia enemmän korroosiota.

Yhteenvetona voidaan todeta, että Prall kulutuskokeet lujittivat käsitystä, että OKTO-murske on hyvin nastarengaskulutusta kestävä materiaali ja SEM-EDS analyysit vahvistivat, että tiepölyssä on OKTO-murskeesta olevaa materiaalia hyvin vähäisiä määriä; näin ollen sillä ei ole osuutta auton osien mekaaniseen kulumiseen, syyt ovat muualla. OKTO-murskeella ei myöskään ole yhteyttä auton osien kloridi-liuosten aiheuttamaan kemialliseen korroosioon.

1 INTRODUCTION

During fall 2013, headline news surfaced addressing the damaged timing belts in certain car models at Oulu region. The mysterious dust found in the car parts was postulated by the national press to originate from the aggregates abraded from the local roads. More specifically, it was attributed to the OKTO-aggregate used in surface wearing course mixtures on high traffic volume roads. The OKTO-aggregate (OKTO-murske in Finnish) is a brand name for the man-made by-product of the smelter slag from the Outokumpu Tornio ferrochromium plant.

Until recently, there has been no method of analyzing road dust that has originated solely from asphalt mixture. However, in the pavement industry, the quality of aggregates and asphalt mixtures are routinely tested against the wear of studded tires. Therefore, the opportunity to utilize unique test equipment available only at the Aalto University Road Laboratory was important motivation for conducting this research.

The test method and equipment typically used to test the wearing resistance of crushed aggregate by industry in Finland is the Nordic Ball Mill test. The Prall test and PWR test (Sivurullakulutus [SRK] in Finnish) are to examine the wear resistance of asphalt mixtures. In addition, a solid aggregate sample can be tested with the SRK apparatus by preparing cylindrical specimens for the test. In all methods, the abrasion value represents the material removed after a fixed amount of applied cycles by the specific wear mechanism of each apparatus.

The Nordic Ball Mill test is conducted on a certain size of crushed aggregates which are abraded by metal balls in the metal cylinder in the presence of water. The aggregates are then classified according to the abrasion resistance; for example, the OKTO-aggregate generally represents a high quality material as being in the best class of A_N7 (the first class). Based on this test, aggregates are selected to be used in asphalt concrete (Finnish Asphalt Specifications: Asfalttinormit, 2011) designed for particular traffic amounts, for example, where the first class is the most suitable for the main arteries and motorways.

On the other hand, asphalt concrete usually consists of not only aggregates, but also of bitumen, fillers and mineral fibers. Therefore, both Prall and SRK evaluate the resistance of the compacted asphalt concrete to wear. These tests are specific to Nordic countries, because of the unique issue of studded tire usage in the wintertime. The Prall test uses bouncing metal balls as an abrasive media in the environment of water. The SRK test consists of a set-up where three small tires with studs on them are cycled around a cylindrical asphalt sample at a fixed temperature and water is provided into the system to remove the abraded fines (Cold regions Pavement Engineering, Dore and Zubeck, 2009).

In this work, it was important to investigate the composition of material abraded from the road by studded tires. Therefore, a decision was made to use the SRK apparatus and to modify it in order to be able to collect the dust. In the normal set-up, the abraded dust is discarded as waste.

2 TESTED MATERIALS

2.1 Tested aggregates and asphalt materials

In this study, we have prepared and analyzed four types of materials, namely: man-made and natural aggregates (solid raw materials), two types of asphalt mixtures (AB16 and SMA22) from two sources, and road dust collected from cars (Table 1).

Table 1. *Summary of investigated materials*

<table>
<tr><th>Material types</th><th>Source</th><th colspan="4">Aalto Road Laboratory</th><th>GTK</th></tr>
<tr><td>AB16 road cores (Reference 1 & 2)</td><td>Mt 837 Utajärvi/ Vittakangas</td><td rowspan="2">SRK abrasion to collect dust from asphalt for further analysis</td><td rowspan="2">XRF, XRD</td><td rowspan="2">FT-IR</td><td rowspan="2">salt</td><td></td></tr>
<tr><td>SMA 22 ICT compacted pills from loose mix</td><td>Vt4 Oulu/Arkala</td><td rowspan="3">FE-SEM and EDS analysis for particle identification</td></tr>
<tr><td>Road dust from cars (Dust 1 to 4)</td><td>Lapin AMK</td><td></td><td></td><td></td><td></td></tr>
<tr><td>Man-made OKTO-aggregate</td><td>PoP ELY/ Outokumpu</td><td></td><td>XRF, XRD</td><td>FT-IR</td><td></td></tr>
<tr><td>Natural crushed rock</td><td>Oulu /Huttukylä</td><td></td><td></td><td></td><td>salt</td><td></td></tr>
<tr><td>Natural crushed rock from South for reference</td><td>Koskekylä, Teisko</td><td></td><td></td><td></td><td>salt</td><td></td></tr>
<tr><td>Limestone and fly ash fillers for reference</td><td>Road Laboratory</td><td></td><td></td><td></td><td>salt</td><td></td></tr>
</table>

The unbound plain aggregates prepared for testing consisted primarily of the man-made OKTO-aggregate and natural crushed rock from the Huttukylä quarry. For the OKTO-aggregate, we decided to use two processing methods for the preparation of fine material to mimic the abraded dust on the road (for FT-IR analysis). The first method involved crushing large diameter aggregate grains in the mill and the second method consisted of wet sieving the aggregates as well as retaining mainly the fraction passing 0.063 mm sieve (fines). These samples are designated as Okto-crushed and Okto-sieved.

Additionally, for the purpose of corrosive tests, we also used Koskenkylä aggregate (widely used in the southern part of Finland), Teisko aggregate, fly ash and limestone for reference.

Asphalt mixtures investigated in this work constituted cored road samples of dense graded AB16 (produced without the OKTO-aggregate) from the Oulu area and the loose SMA22 asphalt mixture with the OKTO-aggregate collected from the overlay construction of VT4 in the summer of 2013 (Nevalainen, 2014).

The loose asphalt mixture was then heated in the oven at 145°C and the cylindrical asphalt specimens were prepared with the ICT gyratory compactor at 145°C with standard SFS-EN 12697-31:2004 parameters using 100 gyrations. Three specimens at the height of 14 cm were compacted and further sawed into an appropriate size for the SRK apparatus (EN12697-16). The specimens need to be at least 45 mm in height with saw cut ends for good gluing adhesion to the sample holders in the apparatus. A total of six (6) SRK-samples were prepared (see Figure 2).

The Lapland School of Applied Sciences (Lapland AMK) provided us with four (4) samples collected from the broken car parts, which were designated by us as DUST1, DUST2, DUST3

and DUST4. Those samples were intended for blind evaluation with similar equipment, thus the detailed origin of the samples was not revealed to Aalto researchers during this project.

2.2 SRK specimens made of loose asphalt mix from VT4

The loose asphalt mix used in the construction of VT4 was designed to comprise 6% limestone filler, 27% of Arkala crushed aggregate fraction 0/11, 27% of the OKTO-aggregate of fraction 11/16 and 40% of the OKTO-aggregate of fraction 16/22.

For verification, one SRK specimen was extracted and gradation determined, see Figure 1. The extracted Sample 6 expressed very similar gradation values to those from mix design reports and it can be concluded that prepared SRK specimens are representative of the asphalt mixture on the road.

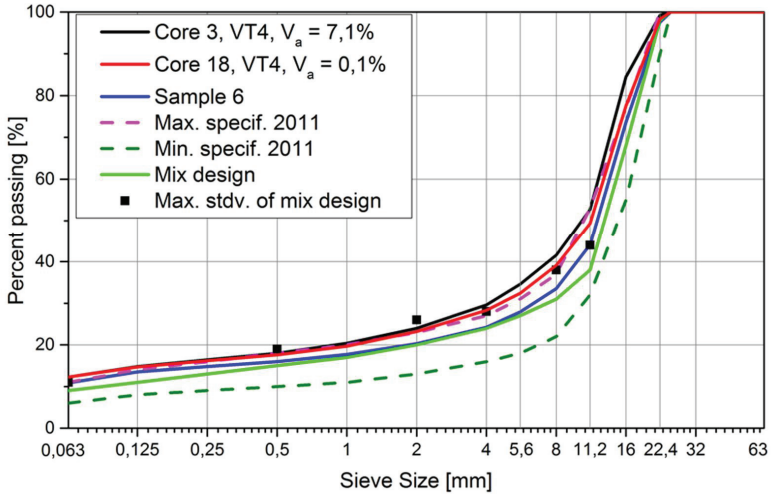

Figure 1. *Gradation analysis for Sample 6 prepared in the laboratory from loose mixture in comparison with Asfalttinormit 2011 gradation envelope for SMA22 (dashed lines) and results from cores drilled from the same road V4 in conjunction of obtaining loose mixture (Nevalainen, 2014).*

As discussed above, the specimens 1-5 were processed according to the procedure described by the standard EN 12697-16. However, as the abrasion values were not the main focus of the project we did not measure it at first. To verify the quality of the asphalt mixture, Sample 5 and reference mixture AB16 Reference 1 were tested for their wear value.

The SRK abrasion value for the SMA22 Sample 5 became 36 ml, placing it in class Abr_{A36}. The measured bulk density of the specimen was 2,674 g/ml, which agrees with the mix design value of 2673 kg/m^3 (EN-12697-6) indicating that the air void content of the specimen was acceptable. The abrasion value for the AB16 (Reference 1) was measured to be 21.2 ml, which places it in class Abr_{A28}, which is better than the sample containing OKTO-aggregate. To understand these unexpected test results, two factors must be taken into account.

By the specification, the SRK abrasion value should be measured from a minimum of three (3) replicated specimens. For the majority of the samples (1-4) tested, visual observation during testing revealed minimal abrasion (see Figure 2) and Sample 5 seemed somewhat exceptional in that sense. On the other hand, the AB16 cores sample (References 1) collected from the road had the diameter of only ca. 94.5 mm, while the laboratory fabricated SRK specimens had a diameter of ca. 100 mm. As the SRK abrasion is created by small wheels rotating around the specimen with these wheels held in place by similarly sized springs, it is obvious that the overly miniscule diameter of the specimen distorts the experiment culminating in an erroneous wear result.

To verify the wear resistance of OKTO-aggregate, a separate testing using a Prall device was conducted according to SFS- EN 12697 – 16 A, which determines abrasion by studded tires, tested on cylindrical specimens abrading the sample with steel balls. Five additional specimens were compacted from the same Vt4 mixture with a gyratory. The obtained Prall values ranged from 12 to 17 ml, the average A_{brA} value being 14 ml. According to Asfalttinormit 2011, the limit for the best Wear-class I is $A_{brA.} < 20$ ml. Overall, the SMA22 mixture containing crushed OKTO- aggregate had thus a very good resistance to the abrasion and, in this regard, will be a valuable material for use on highways.

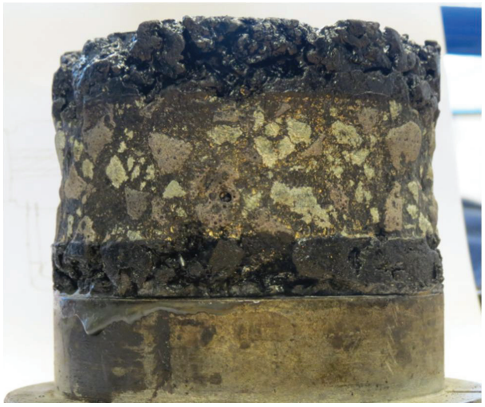

Verification of mixture studded tire abrasion wear class with Prall testing:
SFS- EN 12697 – 16 A
For best Wear-class Abr_{A20} ≤20 ml

Sample	Bulk density (Mg/m3)	Max density (Mg/m3)	Air voids (%)	Abr_A (ml)
1/1	2,683	2,746	2,3	15
1/2	2,682	2,746	2,3	17
2/1	2,697	2,746	1,8	13
2/2	2,680	2,746	2,4	13
3	2,621	2,746	4,5	12
Avg	2,672	2,746	2,7	14

Figure 2. *Left VT4 mixture Sample 3 (with OKTO-aggregate) after SRK abrasion and right results of Prall testing of the same mixture.*

3 EXPERIMENTAL SET-UP

This chapter presents sample preparation techniques and quality control methodologies used to ensure that the prepared samples are representative of the materials in question (Table 2).

Table 2. *Summary of the prepared materials by Road Laboratory.*

Sample ID	Description	SRK wear	Extracted	Salt reaction
Sample 1-4	Asphalt with OKTO	x	By pressure	
Sample 5	Asphalt with OKTO	x	By automatic extractor	x
Sample 6*	Asphalt with OKTO		By automatic extractor	
Reference 1*	Asphalt without OKTO	x	By automatic extractor	x
Reference 2	Asphalt without OKTO	x	By automatic extractor	
Okto-crushed**	Crushed in the mill	n/a	n/a	
Okto-sieved**	Sieved from aggregate	n/a	n/a	

*) SRK abrasion value was measured. **) These samples were prepared for FR-IR reference use.

3.1 Modified SRK equipment

At the beginning of the project, the SRK equipment required modification and cleaning. As discussed above, in a typical abrasion test, the subject is the asphalt sample itself and not the dust, thus the equipment had a build-up of abraded material necessitating a thorough clean of the apparatus. Afterwards, two empty runs were performed to rinse any cleansing agents from the equipment. Figure 3 shows a picture of the cleaned apparatus.

Figure 3. *Cleaned SRK chamber for abrading the fines from SRK-samples.*

The waste water stream was originally connected to the drainage but this had to be modified to collect the dust. We connected the waste stream to a set of three containers designed to capture all of the water with the dust and only the overflow pipe from Container 3 (the last in line) was connected to the drainage (Figure 4). Luckily, the overflow condition was not reached during testing.

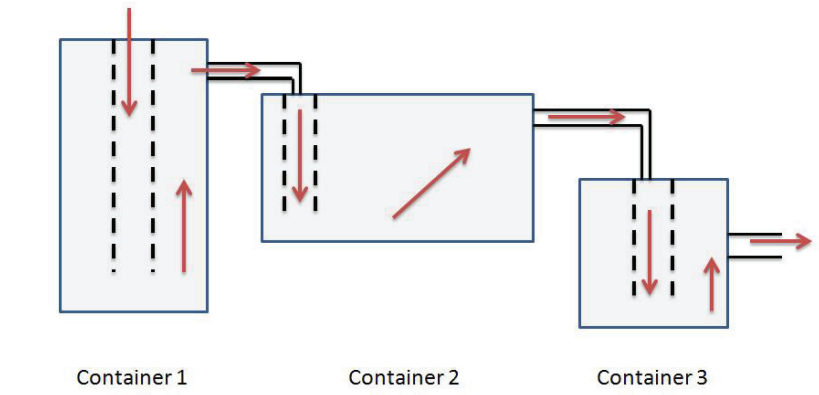

Figure 4. *Waste water collecting system – a) schematic representation, where red arrows indicate assumed waste water flow, b) the actual setup.*

3.2 Methodology used to obtain the abraded dust samples

A standard EN12697-16 Procedure B was applied to condition the samples for the same period of time (2 hours). The water used in the SRK was tap water.

3.3 Methodology of removing abraded dust from water suspension

After the sample was abraded in the SRK, the equipment was stopped and the collected water in all the containers allowed to settle over a 24 h period with the chamber door open and allowed to dry at an ambient temperature.

The fines were collected from three points: inside the equipment (around the magnetic holder of the SRK), inside the equipment (on the bottom tray, walls and doors), and from the water containers. The samples of fines were marked A, B and C, respectively.

The water borne fines had to be separated, but the volume of the liquid was over 240 l. The largest particles precipitated to the bottom of the barrel and the surface liquid (supernatant) remained clear. We removed the supernatant from the container by means of suction from the above precipitate, ensuring the setup was not disturbed, until the passing supernatant started to look cloudy. This point was usually achieved around 4-6 l from the bottom of the container. This liquid was collected for separation as described below. The third container did not usually contain much liquid, and the liquid in it was rather clear. The supernatant was completely removed from it and walls dried.

Due to a lack of previous experience with this system, we applied particle separation procedures which seemed suitable at the time. Unfortunately, we needed to change the method of separation from water suspensions due to its apparent inefficiency. Therefore, Sample 1 is considered a test sample and was not used in later analysis.

The water collection containers were allowed to dry in the laboratory until the wall dust could be removed with a brush (usually 24 h). This dust was further combined with the dust separated from the water and all were marked as sub-sample C.

3.3.1 *Separation of the fines by filtration*

Initially, gravitational filtration was attempted. This was deemed ineffective, as fine particles clogged the filter immediately and further hindered a proper flow of liquid. Filtration in this case lasted longer than time allowed per filter causing a rupture.

We switched to vacuum filtration with a filter of a pore size of 0.002 mm (see Figure 5). The filtration time was faster and the filters did not rupture. However, the filtrate solution was still cloudy (white, non-see-through) after the process, suggesting that some particles went through. At this point, it was not clear if those particles passing the filter were significant. Additionally, it became also problematic to remove the particles from the cellulose filter paper as they clearly clogged the pores and partially remained inside the filter. Therefore, a decision was made to change the separation method.

Figure 5. *Vacuum filtration set-up.*

3.3.2 *Separation of fines by precipitation and drying*

We decided to apply the precipitation method. The liquid from the bottom of the container (containing the majority of fines) was collected into gravitational columns and allowed to precipitate for a period of 72 hours (solution was still cloudy but see-through). An example is shown in Figure 6.

Afterwards, the clean supernatant was removed by suction without disturbing the precipitate. The bottom residue from all columns was then agitated and poured into an evaporating dish, which was placed in the following step into a circulating oven at 110°C until the remaining water evaporated, plus one hour in order to dry the fines. The dish was then placed in a desiccator and allowed to cool.

Such obtained fines were removed from the evaporating dish by means of a spatula and gently pulverized with it. The fines were joined together with the ones collected from the wall of the container and marked “C”.

Figure 6. *Gravitational columns before and after 72 h precipitation stage. The three columns on the left are from the first container and the two columns on the right from the second container.*

3.4 Methodology of cleaning the dust from bituminous residue

The fines collected from water were abrasion residue. They have been analyzed in many cases as is in the Fourier Transform Infra-Red measurement (FT-IR). However, for the purpose of preparing samples for further investigations by the Scanning Electron Microscope (SEM), where an ultra-high vacuum is applied to the sample, the risk of equipment contamination is high, thus advocating cleaning the samples of excess carbonaceous material (capable of evaporation in these conditions).

As bitumen is at least 99% soluble in dichloromethane (DCM), this solvent was chosen as a cleansing agent.

Dichloromethane meant for extractions was used at two qualities: HPLC grade when pressure and the centrifuge cleaning method were applied; and typical industrial quality, when automatic extractor was applied.

3.4.1 *Extraction by vacuum filtration*

Fines were immersed in 200 ml of DCM and allowed to digest with the help of agitation. This mixture was then filtered through the vacuum filtration system (as presented in point 3.3.1.). The sample was washed with portions of DCM until the liquid passing through was transparent.

This was executed on Sample 1 and Sample 2. However, the method was deemed unsafe by the work safety inspector and a decision was made to not continue in this manner with the rest of samples due to the health hazard.

3.4.2 *Extraction by centrifuge wash*

Samples which were provided for fine analysis in GTK (sample 3 and 4) and samples provided by Lapin AMK (DUST 1, 2, 3 and 4) were prepared in the same manner, by centrifuge.

The samples (less than 0.1 g) were dissolved in around 10 ml of DCM and inserted into centrifuge tubes. The tubes were rotated for 12 minutes at 2000 rpm. Afterwards, the supernatant was removed from above the precipitate with a pipette and if the color of the supernatant was not transparent, another wash with the same parameters was performed. Usually three repetitions were needed to obtain a clean product. In the following step, the tubes were placed in the oven, dried at 110 °C and allowed to cool in the desiccator. This prepared product was then transferred into a small glass container with a clean spatula.

The order of processing the samples focused on eliminating particle transfer from the OKTO-aggregate from the dust originating from the cars; thus, following a chronological order, first the DUST samples were processed, followed by the samples prepared in our laboratory.

3.4.3 *Extraction by automatic extractor equipment*

Part of the samples (Sample 5 and 6, Reference 1 and 2) were extracted by an automatic bitumen analyzer, which is a closed system, causing less hazardous situations for the staff handling it.

In this method, fines were poured dry into the extractor apparatus and a standard washing was conducted, where 2 l of industrial grade DCM washed the fines, which were agitated in circular motion. Fines were then collected on the filter paper and transferred into a glass jar by means of a clean brush.

4 ANALYSIS WITH FT-IR

4.1 Fourier Transform Infrared Spectroscopy (FT-IR)

FT-IR is a technique (see Figure 7) in which a wave of infrared light is passed through a sample and recorded by the detector. The infrared wavelength of the light is usually absorbed by the molecules and expressed by means of physical agitation. Each molecule of specific geometry (no two molecules are the same), will possess different energy levels of allowed movement. For example, the molecule can express its movement by symmetrical stretching, anti-symmetrical stretching, scissoring, rocking, wagging or twisting.

Typically, the method is used in the analysis of organic materials, which absorb the wavenumbers between 4000-400 cm-1. However, the minerals and inorganic salts are also known to express the signal in this region, therefore, the method can be used to analyze both organic and inorganic matter. For example, the region of mid-range Infrared covers the light metal salts spectrum. In order to analyze iron and heavy metals, Far-IR (region of lower energy) is recommended.

Figure 7. *FT-IR apparatus at Road Laboratory. In this project, FT-IR was used as a screening and evaluation tool for obtained fines, as well as an evaluator of organic matter contamination.*

As we have shown in (Makowska et al. 2014), FT-IR is also a very useful and fast tool for identifying the composition of asphalt concrete fines. The measurement lasts approximately one minute, can be performed immediately after extraction, and can answer the question whether the mixture contains limestone, hydrated lime or just silica oxide minerals (aggregates and fly ashes). The method is currently used in forensic investigations in many applications, but also, for example, as a tool for identifying the composition of coloring agents used by artists throughout the history of human kind.

4.2 Typical aggregate spectra and information

In our previous studies (Makowska et al., TRB 2014), we have demonstrated methods with which to distinguish between the major asphalt components, namely, limestone filler and granites.

The methodology involves obtaining FT-IR spectra in the Attenuated Total Reflectance mode. The peaks for calcium carbonate and silica are usually dominant in the fine fraction; however, a partial analysis of the Far-IR region between 700-400 cm^{-1} is also possible. In this region, information is located about salts and oxides of heavy metals and can be investigated more closely.

On the basis of the literature review on green pigments containing chromium oxides, we were able to determine that the region between 700-600cm^{-1} contains information connected with chromium compounds, thus we chose it as an identification region for the OKTO-aggregate samples.

Table 3. *Wavelength values with assigned minerals (data collected from literature).*

Literature [reported values]	Wave-number [cm^{-1}]	Compound assigned
Akyuz et al. (2012)	668	*gypsum
	632, 637, 692	Chromium compounds
Vahur et al. (2010)	629w, 579 w	Chrome oxide green
	678	*Viridian green (chromium oxide dihydrate)
Makowska et al. (2014)	711, 874 ,1420	Carbonate
	754, 728	Albite
	1166, 1008, 664	Silica

4.3 Methodology

Collected fines or collected and extracted fines were dried in the oven at 110 °C in order to remove absorbed water. Samples were cooled down in the desiccator. The spectra were collected at 25 °C in ATR/Transmittance mode. Usually a spectrum of the sample before and after extraction was obtained.

The reference material of OKTO-aggregate was prepared by two methods. One involved sieving the coarse aggregate and collecting only the material (fines) passing 0.063 mm sieve, whereas other involved crushing coarse aggregate in the mill and analyzing obtained dust.

As one of the reference samples we have also analyzed the spectra of fines extracted from SMA22 (with OKTO-aggregate), which are passing 0.063 mm sieve (Sample 6).

4.4 Results and analysis

In Figure 8 we have plotted representative spectra of raw material references.

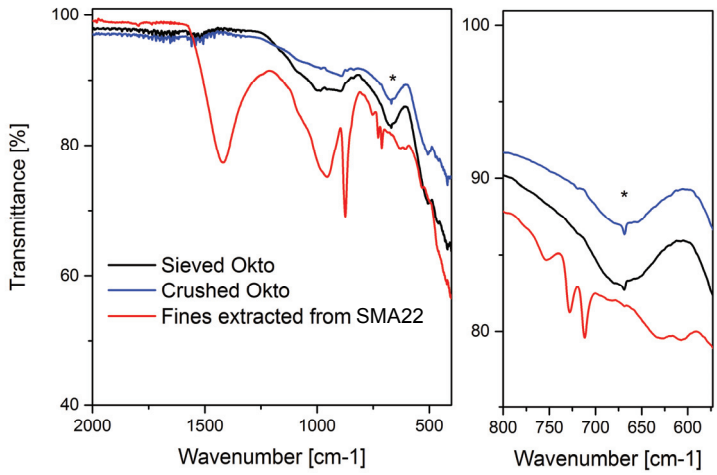

Figure 8. *FT-IR ATR spectra of OKTO-aggregate fines compared with the spectra of fines passing 0.063 mm sieve extracted from SMA22 sample containing OKTO-aggregate.*

As can be observed in Figure 8, with respect to Table 3, the aggregate sample extracted from SMA22 mixture clearly expressed peaks characteristic of calcium carbonate and silica. Seemingly, the crushed OKTO-aggregate does not contain calcium carbonate, but on the contrary expresses a characteristic silica feature (flat with two maximums) alongside the peaks in the more Far-IR region characteristic of heavy metals and especially chromium oxides. On the basis of the previous work cited in Table 3, we can assume the presence of gypsum or chromium oxides with the characteristic feature at the wavenumber 668 cm^{-1}. The broad peak in the region 600-750 cm^{-1} might be due to the different forms of chromium compounds contributing at once to the spectra.

Figure 9 compares reference samples with the SRK-abraded dust. The upper plot has SMA22 mixture with OKTO-aggregate (Sample 3), whereas the lower plot has AB16 mixture without OKTO-aggregate (Reference 1). Figure 9 reveals that although a similar characteristic feature at 668 cm^{-1} (sharp small peak) is expressed in reference samples, the decrease in Transmission in the 600-750 cm^{-1} is not observed at the same time. However, this decrease in Transmission in that region (broad peak) is somewhat characteristic of samples containing the OKTO-aggregate. Additionally, no calcium carbonate characteristic peaks were found in the abraded fines of AB16 (Reference 1), which is consistent with reported mix design (Figure 9 lower spectra).

In terms of screening analysis, we were able to find that less water borne fines (Samples 1-5 A collected from inside the SRK equipment) contained small amounts of calcium carbonate, whereas samples C, collected from water containers contained a vast amount of this component alongside water borne silica. We observed that chromium compounds were evenly

distributed between the fines A, B and C. On the basis of this analysis, it was determined that the most representative samples for the additional analysis of salt reaction were the B samples, which were obtained inside the SRK equipment by collecting dust from the bottom tray, walls and doors.

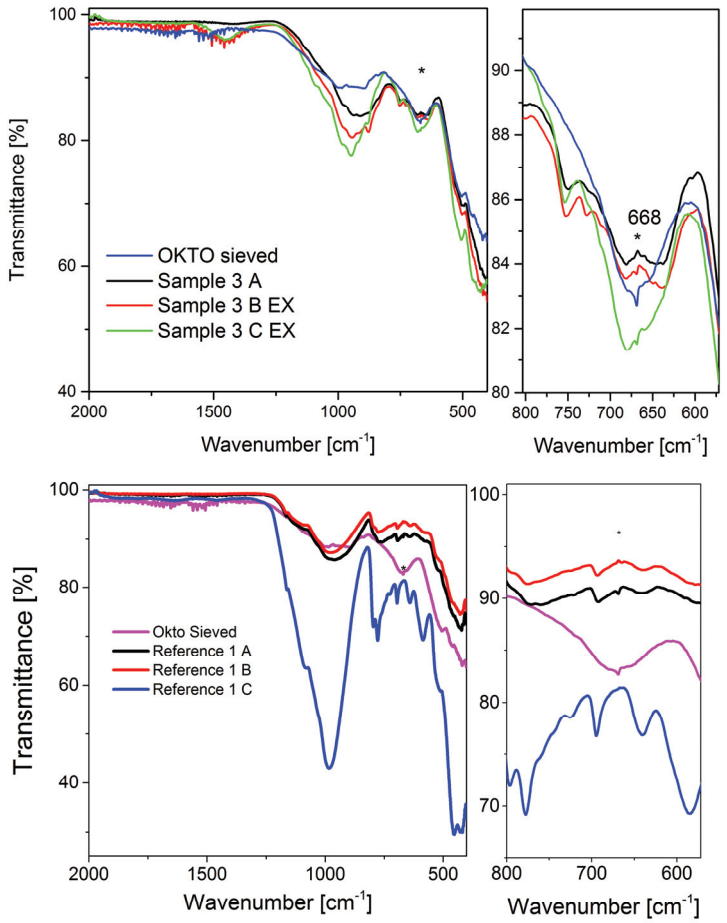

Figure 9. *(Upper) An FT-IR ATR spectra of fines obtained from abrasion of SMA22 samples with OKTO-aggregate; (Lower) spectra obtained from analysis of fines abraded from AB16 (Reference 1) without OKTO-aggregate.*

With the FT-IR, we were able to establish that there was no exceptional behavior between the individual samples, a similar separation pattern was observed during a screening analysis in all the five experiments conducted on prepared SRK samples 1-5, and as such these experiments were deemed as being repeatable.

5 INVESTIGATIONS WITH XRF AND XRD

The XRF-analysis was executed to evaluate fines extracted from the asphalt mixture and to quantify the OKTO-aggregate itself. Therefore, before carrying out a more detailed SEM-EDS analysis, the composition of the supplied OKTO-aggregate, samples was compared with its bulk properties described in the commercial Material Safety Data Sheet (Outokumpu, 2013). The analysis was done using X-ray fluorescence (XRF) and diffraction (XRD) methods on visually selected aggregate fragments ranging about 1-1.5 cm, which were then subsequently pulverized for further analysis. These were analyzed using a hand-held Thermo Scientific Niton XL3t XRF Analyzer. Taking into account the analytical precision of this field-measuring device, the composition of fragments extracted for investigation is consistent with the average composition of the bulk material specimen of OKTO-aggregate as defined by the manufacturer.

5.1 OKTO-aggregate

The OKTO-aggregate consists mainly of slag material of the ferrochrome smelting process. Besides amorphous silicates and oxides as major components, it includes the accessory crystals of chromium containing spinel-group minerals and Mg (Cr)-silicates representing residual minerals from enriched ore and crystals formed in the metallurgical processes. A comprehensive detection of all minor crystalline phases was not attempted, but, generally speaking, observations made with the XRD were found to be consistent with the material safety data sheet. The results confirmed that besides amorphous silicates and oxides as major components, it included crystalline phases, such as forsterite (Mg2SiO4, aka Mg-olivine) and spinels, Al-Mg- and Mg-silicates, and metal oxides. The diffractogram is provided in Appendix A.

The hand-held XRF Analyzer (see Figure 10) is a portable field instrument that can be used for an analysis of both solid and powdered samples with detection limits that are typically less than 0.05 %. The limitations of this technique result in an inability to analyze the light cations, such as sodium (Z less than 11) and oxygen. Therefore, their contribution must be deduced from the overall mass balance. In addition, the type of sample matrix affects the results and different types of samples require specific settings and calibrations to the standard samples.

Figure 10. *Demonstration of XRF testing and sample preparation.*

The XRF apparatus analyzes the volume of a sample which is about 1 cm in diameter and a few millimeters thick. Therefore, the analysis is prone to variation due to heterogeneities. Consequently, the comparison of the results to analytical results obtained by different sampling protocols, sample sizes and analytical methods should be carefully executed. The results involve uncertainties, which have been approached in ore grade control and mineral processing under the concept of fundamental sampling error (Gy, 2004). The composition of the obtained OKTO-aggregate material from Oulu was compared with its bulk properties described in the report by Jokinen (2002) and the Material Safety Data Sheet (Outokumpu, 2013). These data represent the averages of laboratory analysis but no information about the standard deviation or other statistics has been given.

The OKTO-aggregate raw material sample comprised ca. 20 kg of aggregate fraction of 10/16 mm. The composition of this sample was assessed using three approaches. First, a bulk sub-sample of about 0.3 kg was extracted and crushed using a standard Proctor device. Before crushing the aggregate, a lump of pure quartz was crushed with the device, all the dust was carefully removed from the chamber and the hammer; finally, metal surfaces were wiped clean with alcohol to remove any particles and residual moisture from the metal surfaces. Specimens of crushed OKTO-aggregate were prepared and the sampling system calibrated according to instructions in the device manual. This sample is designated as OKTO (Proctor).

The second approach to preparing the sample was to extract fines from the OKTO-aggregate by wet sieving material without any other preceding handling procedure. This sample is designated as OKTO (sieved). The third sample was obtained by shaking the Proctor crushed OKTO-aggregate described above in a bowl and manually selecting ca. 1mm grains to be further ground by hand in an opal mortar. This sample is designated as Okto- (crushed). Table 4 shows the XRF results.

Table 4. *XRF- results (units mass-%) for fines obtained from pure OKTO-aggregate*

Source/ ID	Fe	Cr	Ca	K	Al	Si	Mg	Bal	sum	sum-bal
OKTO-(Proctor) 1	2.55	4.54	0.67	0.15	2.07	6.33	0.00	81.07	98.08	17.01
OKTO-(sieved) 2	15.0	7.8	1.6	0.6	6.1	12.6	3.2	55.1	101.9	46.8
OKTO-(crushed) 3	8.7	4.0	12.7	0.3	3.5	9.9	2.1	62.1	103.3	41.2

Comparison of the crushed OKTO-aggregate material suggests at first that our sample has lower than the main cation concentrations compared to reported OKTO-aggregate material. However, the comparison of fines extracted from the uncrushed and crushed OKTO-aggregate used as references in the SRK analyses indicated that some of the obtained metal concentrations in fine fractions are higher than that of the bulk OKTO-aggregate composition. These observations suggest that analysis of the bulk composition of the OKTO-aggregate might be a question of variation of compositional fractionation during grinding and biased sampling during the splitting of sub-samples. In the case of the porous material, such as the OKTO-aggregate, the standards available may not be ideal for the porous Fe-Mg rich material.

In order to assess statistically how representative and homogeneous the supplied OKTO-aggregate material was, 16 initially picked random grain particles were measured and the Mean and the Standard deviation of the results were determined (see Table 5). The total mass of the analyzed particles was 113.5 g. In general, the standard deviations ranged from 0.16 to

3.6 % for K and Mg respectively. The 95 % confidence intervals for the analyzed OKTO-aggregate grains were lower for Fe, Cr, Mg and Ca compared with the reported OKTO-aggregate concentration (Outokumpu, 2013). On the other hand, the concentrations of Al and K are higher while Si concentration is the only main component for which 95% confidence interval contains the reported concentration. Consequently, the measured grains are enriched in terms of the heavier elements and somewhat depleted in light elements compared to the reported OKTO-aggregate composition.

Table 5. *XRF results (units mass-%) for OKTO-aggregate grains (10/16 mm).*

Source/ID	Fe	Cr	Ca	K	Al	Si	Mg	Bal	sum	sum-bal
Material Safety Data Sheet	4.0	9.0	1.4	0.0	13.8	14.0	13.9			56.1
OKTO-grains, **Mean**	2.1	6.1	0.99	0.23	9.7	15.4	8.4	55.4	98.5	43.1
OKTO-grains, **Stdev**	0.73	1.3	0.2	0.16	3.5	3.5	3.6			

5.2 Fines obtained from asphalt mixture

The XRF-analysis was also used to quantitatively analyze the SRK-samples and reference samples of fine materials discussed in Chapter 4.3. In Table 6, samples SRK 1AB to 5C correspond to fines extracted via SRK abrasion from asphalt samples. A reference sample of asphalt fines was obtained after bitumen was dissolved by dichloromethylene (Sample 6 prepared without SRK abrasion). The residual solid material is a mixture of 6% calcium carbonate filler, 27% natural rock aggregate, and the rest is OKTO-aggregate according to the mix design. The material passing 0.063 mm sieve was analyzed. In that fraction, according to the mix design, calcium carbonate or limestone should consist of 90.6% of that sample and 8.8% should be characteristic of the Arkala aggregate, while the rest (0.6%) is OKTO-aggregate. As Table 4 shows, the reference Sample 6 has less Fe and more Ca as it does not contain abraded OKTO-aggregate from the larger grains.

Table 6. *XRF results (units mass-%) for fines extracted from SMA22 asphalt.*

Source/ ID	Fe	Cr	Ca	K	Al	Si	Mg	Bal	sum	sum-bal
SRK 1AB	4.4	3.5	6.7	0.1	3.3	12.3	1.6	66.5	98.4	31.9
SRK 2B	4.7	4.3	5.9	0.1	3.4	12.1	1.3	66.8	98.6	31.8
SRK 2C	4.6	4.6	5.7	0.1	4.1	12.4	1.6	65.7	98.9	33.2
SRK 3B	5.1	3.8	6.5	0.1	3.2	11.5	1.3	66.9	98.5	31.6
SRK 4B	4.1	5.1	5.4	0.1	4.1	12.3	2.1	65.4	98.9	33.4
SRK 4C	3.6	4.7	5.1	0.2	4.6	13.6	2.6	64.2	98.6	34.4
SRK 5B	4.3	4.9	6.5	0.1	4.1	12.9	2.6	63.5	99.0	35.5
SRK 5C	4.8	3.8	5.2	0.1	2.6	9.6	0.0	71.9	98.0	26.1
Sample 6 (<0,063 mm)	2.4	0.2	23.8	0.1	1.0	7.2	1.0	69.2	104.7	35.6

6 ELECTRON MICROSCOPIC STUDIES

In order to more precisely distinguish possible fragments derived from OKTO-aggregate, investigations were continued with the field emission electron microscope. Consequently, polished sections were made of two visually selected fragments of OKTO-aggregate. A portion of each of the five dust samples obtained in SRK-tests and four anonymous dust samples (DUST1, DUST2, DUST3, DUST4) representing four different car models from the Oulu region were also prepared for electron microscope studies.

In scanning electron microscopy (SEM), the surface of the sample is bombarded with an electron beam in a vacuum. In field emission (FE), the facility enables focusing and the control of the electron beam allowing the imaging scanning to be done at a resolution of 1-10 nanometer (Reimer 1998). The application of the electron beam produces x-ray emissions which enable the distinction of elemental contents using energy dispersive spectrometry (EDS). EDS-analyses can be used to detect most elements with a precision of about 0.5 w%. On polished surfaces, the intensity of electron backscattering (BSE) is proportional to the average atomic numbers in the solid phases. Most minerals can be distinguished based on their gray scale tones in BSE-images. For cases when the mean atomic number is similar, the distinction of different solid phases can be done using EDS-analysis besides image processing of BSE measurements (Vaughan & Wogelius 2000). Analytical software applications have been developed for FE-SEM-devices for the automatic distinction and analysis of mineral phases, as well as for the classification and quantitative analysis of particle size distributions. The results analyzed in the following were obtained in a Finnish geoscientific research laboratory with Jeol JSM-7001F FE-SEM and Oxford Inca Features software.

6.1 Elemental point analysis and distribution maps

EDS-point analysis gives an estimate for a composition within an area of about 10 μm in diameter. Therefore, they do not necessarily provide estimates for the different phases in the sample but for the average composition of the area analyzed. The results of the analysis were done solely to guide the automatic particle analysis as the following step of the investigation was to classify fragments in the samples.

The results of the point analyses are given in Appendix B; although the results are not intended for quantitative and conclusive comparisons of the different samples, they provide information about the composition of the different phases in the fragmental material. Based on the point analytical results, the key findings are as follows:

- The samples from the damaged cars also include a small but significant concentration of chloride ranging from 0.5- 10 %. Chloride is associated with Fe and does not correlate in any way with Na, Ca or K. Therefore, the chloride likely occurs as $FeCl_3$ associated with Fe-oxides and Fe-oxyhydroxides (rust).

- The metal rich point analyses in different samples vary in terms of Co, Cu, NI and Zn concentrations associated with Fe.

- Only a few sporadic points from car dust contain chromium. For example, samples DUST2 and DUST4 contain two points out of 72.

The elemental distribution maps of OKTO-aggregate microscope samples were done using EDS-analyses in a continuous mode. In the maps, the concentrations of different elements are given as the intensity of a certain color as is shown in Figure 11. These illustrations show that at the micro scale, OKTO-aggregate is heterogeneous material comprising essentially glassy amorphous parts of Ca-Al- and Mg-silicate composition, and parts comprising Mg-Mn-Al-oxides. The texture can range from angular fragmental texture (as in Figure 12) to one with gradational contacts giving the appearance of partial mixing and welding of molten material due to a viscous flow. Chromium is detectable in all different compositional zones but the concentration varies. High concentrations can be found in iron blobs also containing 8-9 % Cr and about 1% Ni. The samples also contain chromium sulfide which is likely an artificial product of the smelter process. Chromium sulfide components are not known to exist in nature and are only detected in certain meteorites (Ma et al. 2010). The amounts of sulfides appear sufficiently small (less than 1 % as informed in the Material Safety Data Sheet) that they do not prevent the use of OKTO-aggregate as an aggregate material (Finnish Asphalt Specifications 2000, 2011). Neither is the presence of observed quantities likely to lead to significant releases of acidic leachates when material comes into contact with water or issues of environmental concerns for which the material has been widely tested (Outokumpu, 2013).

6.2 Detection of OKTO-aggregate from asphalt samples (SRK-samples)

The next step was to carry out a study by FE- SEM on the SRK-test dust and the car dust as well as to distinguish particles that could be derived from the OKTO-aggregate. The automatic distinction of features is partly based on BSE-grayscale image interpretation, which depends on the average atomic weight of the material, and partly on the chemical composition defined by EDS-analysis. A feature in this analysis means a compositionally sufficiently homogeneous area that can be delineated based on the BSE distribution and/or EDS-analysis. A particle can comprise one or more features. In the case of a particle abraded from rock or, in general, derived by the mechanical breaking of rock, it can consist of a single mineral (e.g. quartz) or comprise two or more minerals which can be distinguished as features. Moreover, existence of small amounts of chromium and tiny chromium containing iron blebs is a characteristic feature of OKTO-aggregate microscope samples. Such detectable features as shown in Figure 11 and Figure 12 can be taken into account in the particle analysis. Furthermore, the software available (Oxford INCA Features) has a substantial database of mineral characteristics, including chemical composition and morphological features, which were used to distinguish typical rock forming minerals in the particles.

Some of the minerals included in the database have essentially the same composition as some of the glassy compositional zones in the OKTO-aggregate material. Therefore, some of the features representing the OKTO-aggregate material have been classified automatically as minerals because they possess a similar chemistry and average atomic weight. Nevertheless, such particles may lack the ordered molecular structure (crystal lattice) that is a key definition of a mineral. An example is fragments of chromium containing Mg-Al-silicate glass which have been “distinguished” as apparent Cr-pyrope fragments. Similarly, particles of the asphalt concrete can be interpreted as clinozoizite, which are likely glassy fragments with an analogical Ca-Al-silicate composition.

The results presented in Table 7 for one of the SRK-test samples suggest that about 39 % of the particles are derived from the OKTO-aggregate, while in the aggregate blend, the natural aggregate proportion has been about 67 %. The main rock aggregate in the test sample is

Arkala amphibolite in which the main minerals are plagioclase and amphibole minerals with minor quartz. The total percentage of features comprising these major minerals of Arkala rock aggregate is about 44 %, whereas in the aggregate blend the proportion has been about 27 %. The total percentage of calcite and dolomite is about 4 % which is consistent with the amount of calcareous filler and its impurities in the aggregate blend (6 %). The remaining proportion of the fragments constitutes either the minor minerals of amphibolite or main minerals of accessory rock types (e.g. granitic veins) in the aggregate production site. The results suggest that the man-made OKTO-aggregate has a better stud wear resistance than the natural rock aggregate material.

Table 7. *Results from automatic particle tracking and analysis of features of SRK-sample (Clean 5.2.14C). Fragments likely derived from OKTO-aggregate are marked with bold text.*

Clean 5.2.14C Feature analyysi (FE SEMillä)

Class	Rank	Features	% total features	Feature area (sq. µm)	% total Feature area
Cr-rich Spinel	4	565	13.4	8030.0	12.4
Spinel	4	472	11.2	6570.0	10.1
Fe-Hornblende	2	471	11.1	6940.0	10.7
Plagioclase	1	433	10.2	7070.0	10.9
Actinolite	2	306	7.2	5110.0	7.9
Mg-Hornblende	2	273	6.5	3310.0	5.1
Chlorite	2	239	5.7	3660.0	5.7
Chrysotile	3	217	5.1	3630.0	5.6
Mg Olivine	3	178	4.2	3070.0	4.7
Cr-pyrope	3	176	4.2	2780.0	4.3
Calcite	4	131	3.1	2330.0	3.6
Slag Cr	6	126	3.0	2160.0	3.3
Albite	1	119	2.8	1830.0	2.8
Quartz	1	118	2.8	2420.0	3.7
Slag1	6	90	2.1	1440.0	2.2
Fe rich carbonate	6	86	2.0	1170.0	1.8
Chromite	4	72	1.7	997.0	1.5
Dolomite	4	65	1.5	715.0	1.1
Clinozoisite	3	14	0.3	327.0	0.5
Mg-biotite	2	10	0.2	226.0	0.3
Cr-steel	6	8	0.2	106.0	0.2
Fe-Cr ox	4	7	0.2	92.3	0.1
Diopside	3	7	0.2	74.8	0.1
K-fsp	1	7	0.2	97.8	0.2
Metallic Fe	6	6	0.1	68.1	0.1
Sphene	3	5	0.1	63.9	0.1
Muscovite	2	4	0.1	62.5	0.1
Ilmenite	4	3	0.1	40.2	0.1
Antigorite	3	3	0.1	40.9	0.1
Talc	3	3	0.1	74.4	0.1
Anthophyllite	2	3	0.1	81.8	0.1
Ni-Cr steel	6	2	0.0	26.1	0.0
Al + S (2nd)	6	2	0.0	28.3	0.0
Fe-ox + S	5	2	0.0	17.5	0.0
Tremolite	2	2	0.0	30.7	0.0
Cu-mineral	5	1	0.0	12.9	0.0
Fe-ox (magnetite/hematite)	4	1	0.0	8.0	0.0
Olivine	3	1	0.0	8.9	0.0
Epidote	3	1	0.0	17.5	0.0
Biotite	2	1	0.0	18.7	0.0
		4230	100.0	64756.4	100.0

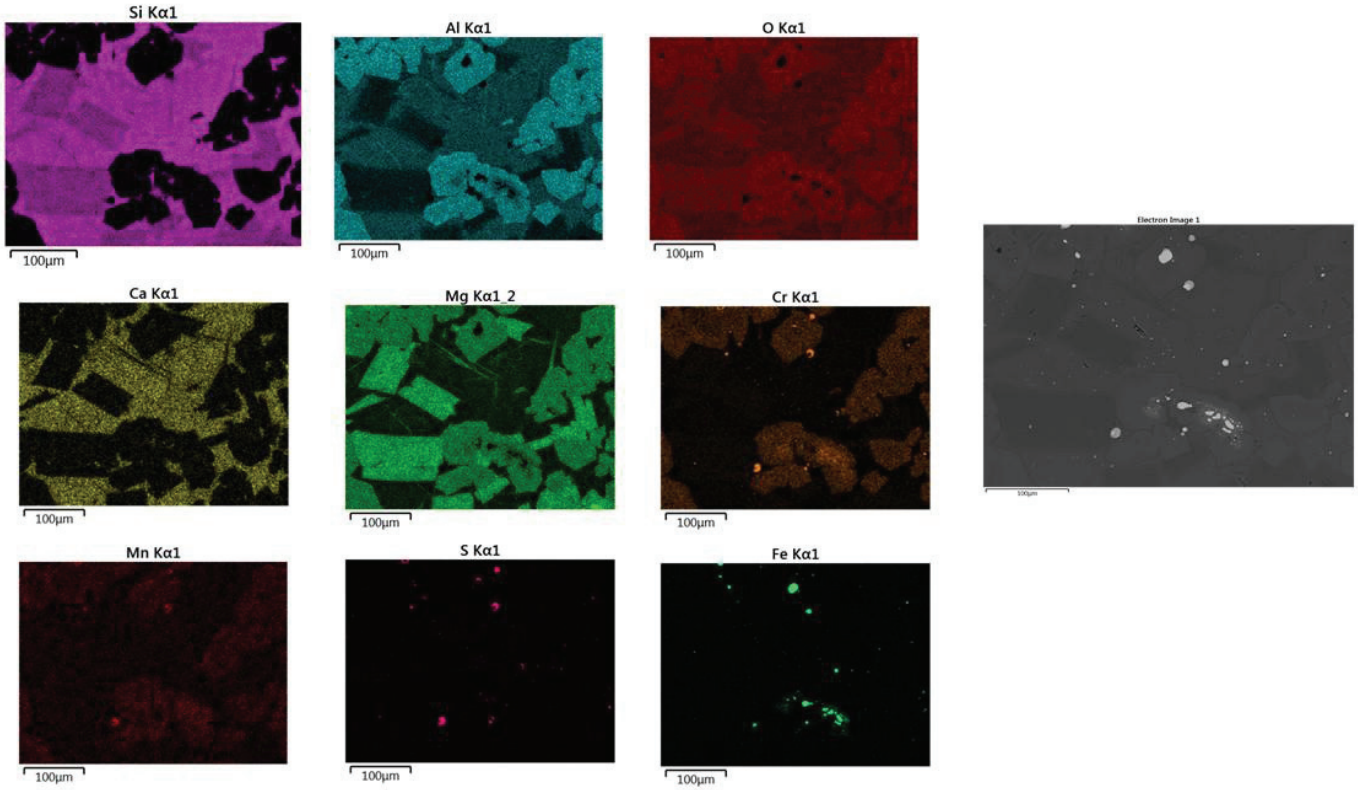

Figure 11. *Compositional maps of an OKTO-aggregate sample based on energy dispersive spectrometry analysis made using an electron microscope.*

6.3 Detection of OKTO-aggregate from car dust

Finally, similar techniques and particle identification settings as in the SRK-samples were then applied to distinguish the OKTO-aggregate-derived particles in samples (DUST1, DUST2, DUST3, DUST4) from the car dust and smear found with the damaged timing belts of camshafts in cars. Examples of detected fragments in car dust samples are show in Figure 12. Consequently, the OKTO-aggregate fragments were considered comprising of Cr-spinels, chromite, Cr-containing iron oxides and iron fragments, and various slag-fragments with a corresponding chemistry to compositional zones observed in the polished sections of the OKTO-aggregate.

The number of particular features classified in each of the four car dust samples ranged from 4851 to 5428. The results of the classification are summarized in Table 8. The number of OKTO-aggregate fragments ranged from 7-23 representing only 0.02-0.1 % of the total area of classified features.

In three samples (DUST1, DUST2 and DUST3), the overwhelming portion of fragments was iron oxides (Fe_2O_3, FeOOH or Fe_3O_4) comprising 4124-4421 fragments that represented 71.7-86.5 % of the total area of features. In these samples, the next prominent features represent different typical rock forming minerals based on their energy dispersive spectrum and composition.

The sample DUST4 contained 798 iron oxide fragments that comprised 11.6 % of the total area of classified particles. In this case, rock forming minerals comprise the highest group (4240 identified features) comprising 85.2 % of the total feature area.

The iron-oxide materials are likely derived from the abrasion and corrosion of the metal parts or represent the filler material in the rubber of the damaged timing belts. More interestingly, all the samples of damaged car engines also contain corundum. The number of corundum particles ranged in the car dust samples from 4 to 383 or 0.004-0.1 % of the total classified particle area. As a very hard mineral (hardness 9 in the Mosh scale), the corundum is commonly used in cutting blades or as an abrasive or polishing material. It is also used as a filler material to improve the thermal conductivity of plastic filler pastes and rubber. The most commonly industrially used corundum is of artificial origin. In the geological setting characteristic of Finland, corundum is a very rare mineral in general and the Oulu region lacks any known occurrences in the geological databases of GTK. Therefore, corundum is likely derived from an artificial source which cannot be defined any more precisely with the present information.

A similar analysis of features was conducted on a microscope sample, Clean 5-2-14C, representing the SRK-dust made from OKTO-aggregate material. Among the 4230 fragments were 1518 and 2711 fragments that were identified as the fragments of OKTO-aggregate and common rock forming minerals, respectively. Only one iron-oxide (no Cr-associated) and no corundum were present. It was concluded that corundum in the car dust samples is not derived from OKTO-aggregate.

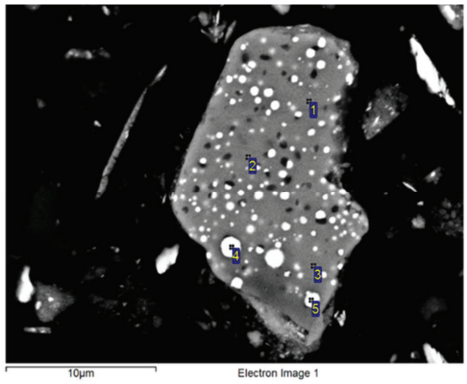

Spectrum	In stats.	O	Mg	Al	Si	S	Cr	Fe	Total
1	Yes	41.10	14.15	8.11			34.42	2.22	100.00
2	Yes	41.02	13.03	8.22			35.79	1.95	100.00
3	Yes	39.59	12.03	7.88			35.04	5.47	100.00
4	Yes	8.52	2.87	1.88	0.76		6.14	79.82	100.00
5	Yes	16.87	5.39	4.10	0.53	0.44	10.28	62.39	100.00

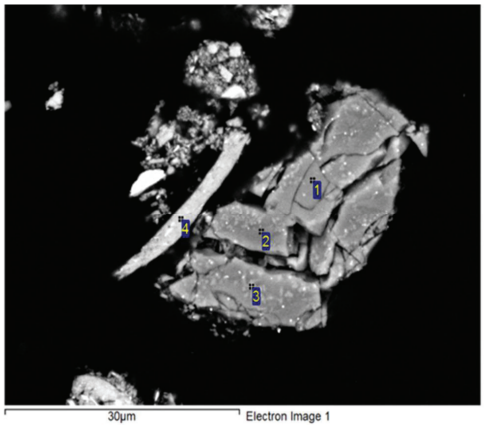

Spectrum	In stats.	O	Mg	Al	Si	S	K	Ca	Ti	Cr	Mn	Fe	Total
1	Yes	49.94	5.21	10.82	26.87		1.05	4.06		2.05			100.0
2	Yes	47.22	27.52	2.70	20.94					1.62			100.0
3	Yes	41.48	7.10	13.02	11.06	8.44	0.51	1.16	0.43	15.04	0.89	0.88	100.0
4	Yes	30.79			1.49							67.73	100.0

Figure 12. *An example of the characteristic textures of a fragment of OKTO-aggregate and EDS-point analyses (in sample DUST1 of car dust). All results in weight %.*

Table 8. *Summary of the feature analysis of the particular samples from the damaged cars (DUST 1 to 4) and from the SRK-dust sample.*

Sample ID	Features	number	% number	% area
DUST 1	Fe, Fe-oxides, Fe-oxyhydroxides	4124	79.64	75.7
	Mineral fragments	1037	20.03	24.1
	OKTO-aggregate	11	0.21	0.1
	Corundum	6	0.12	0.05
	Total	5178	100.00	100.0
DUST2	Fe, Fe-oxides, Fe-oxyhydroxides	4295	85.07	71.7
	Mineral fragments	687	13.61	27.1
	OKTO-aggregate	23	0.46	1.0
	Corundum	44	0.87	0.3
	Total	5049	100.00	100.0
DUST3	Fe, Fe-oxides, Fe-oxyhydroxides	4421	91.14	86.5
	Mineral fragments	410	8.45	13.0
	OKTO-aggregate	16	0.33	0.5
	Corundum	4	0.08	0.02
	Total	4851	100.00	100.0
DUST4	Fe, Fe-oxides, Fe-oxyhydroxides	798	14.70	11.6
	Mineral fragments	4240	78.11	85.2
	OKTO-aggregate	7	0.13	0.07
	Corundum	383	7.06	3.2
	Total	5428	100.00	100.0
SRK 5 (Clean 5-2-14C)	Fe, Fe-oxides, Fe-oxyhydroxides	7	0.21	0.1
	Mineral fragments	2711	63.90	60.4
	OKTO-aggregate	1518	35.89	39.5
	Corundum	0	0	0
	Total	4230	100	100

7 REACTIONS WITH SALT

7.1 Review of impact of deicing chemicals and theory

This chapter discusses the reactivity of iron chloride, reactivity of calcium chloride, sodium chloride and the use of deicing chemicals in the Oulu region.

If the dust was consistent with road dust, and OKTO-aggregates are used in that area, there is no reason to believe that traces of the OKTO-aggregate would not be found in it. The road dust is formed from a blend of deicing chemicals and particles abraded from the road by the action of studded tires combined with impurities from air. Thus, it is an implausible scenario in which no trace of chromium would be found in the road dust derived from the area where the OKTO-aggregate is used. The only plausibility of this occurring is if the OKTO-aggregate has undergone a galvanic reaction with deicing salts, leading to an abrasion of particles not containing chromium. Even in such case, traces of the initial ore should be identifiable. On the basis of such strongly presented data where "no chrome at all" was reported by the press, it was postulated by the authors that the dust must have an origin in the back splashing liquid from the road, which would contain only water soluble components. According to galvanic series (of corrosiveness of metals in salt solutions), it is known that in an environment where chrome is present, no chrome will transfer into such a solution of brine. On the basis of this fact, it was suggested that the behavior of the OKTO-aggregate be tested in the deicing solutions.

During our study it was identified that in the region of Oulu, the use of deicing chemicals is divided between sodium chloride (NaCl) and calcium chloride ($CaCl_2$). Based on prior research, it is known that calcium chloride is twice as corrosive as sodium chloride at similar concentrations. We investigated if the maintenance use of this chemical was somewhat exceptional in the region. Table 9 presents the results provided by ELY centers. Indeed, there is a much higher use of calcium chloride in the region than in some other regions of the country, but the amounts used are not exclusive to the Oulu region (PoP ELY).

Table 9. *The use of calcium chloride for winter maintenance in Finland.*

	1.10.2007-30.9.2008			**1.10.2012-30.9.2013**		
	Salt applied (t)	Solution $CaCl_2$ usage		Salt applied (t)	Solution $CaCl_2$ usage	
		(t)	%		(t)	%
UUD ELY	29562	493.4	2	27015.3	252.1	1
VAR ELY	11788.8	326.7	3	11309	186.4	2
KAS ELY	11830.1	541.2	5	5876.5	0	0
PIR ELY	8136.6	1443.1	18	7774.7	1071.3	14
POS ELY	10122.8	1650.5	16	7710.5	965.3	13
KES ELY	6737.3	1710.1	25	4652.2	159.9	3
EPO ELY	9710.4	2627.8	27	7019.6	268.5	4
POP ELY	8551.5	725.1	8	6306.1	477.4	8
L ELY	2027.3	122.2	6	2199	52.8	2
Whole country	98466.8	9640.1	10	79862.9	3433.7	4

In earlier research (Vestola et al. 2006), it was pointed out that the activity of calcium chloride as a corrosive agent is significantly affected by moisture at various temperatures. Sodium

chloride works slowly in conditions below 76% moisture in the air in temperatures between 0 and 25°C, whereas this value drops for calcium chloride from 45 to 30% moisture, between 0 and 25°C respectively. If the deicing chemicals were responsible, the growth of occurrence should be observed during the spring time, when roads and road dust still contain deicing chemicals, but both the temperature and moisture will have increased above these critical values for calcium chloride.

Calcium chloride, which allows for the salting solution to work in temperatures as low as -50°C, is rarely used in countries with a warm climate and, therefore, perhaps its effects are not as well known. It is also a compound which is absorbed by the environment much faster than sodium chloride, and as such is more environmentally friendly. Currently, its increasing price limits the use to only necessary situations and places, such as those reported in Finland.

7.2 The effect of preceding analysis on the applied methodology.

After assessing results between Aalto University and Lapin AMK, it became evident that the OKTO-aggregate traces were found in the dust by both parties, as opposed to results reported in the press. Therefore, it became obsolete to prove the postulate for the galvanic series.

Additionally, the locality of the occurrence of car damages suggested by the press was not confirmed in this study. Until proven otherwise, it is fair to assume that similar damages can and are occurring elsewhere.

However, Aalto University identified one of the main components of the dust as iron (III) chloride. The origin of this compound can be traced as originating both from corroded steel, but also from corroded aggregates. The work was divided between Lapin AMK and Aalto University to test these two possibilities of origin.

Iron (III) chloride is both a product of corrosion, but also a mild corrosive agent itself (Rautakloridi, kemikaalikortti). Iron (III) chloride is a known catalyst of the polymerization of styrene and other polymers (Cai et al. 2007), thus, perhaps its presence has a subsequent effect on the damage of the belt (typically made of styrene-butadiene rubber). If some particular aggregate would release more of this agent, it would be plausible to claim that transfer from such road dust enhanced normal car part corrosion.

Aalto University investigated the behavior of aggregates in acidified solutions of brines, whereas Lapin AMK investigated the behavior of the gear in brines.

According to the previous work (Vestola et al. 2006), calcium chloride is more corrosive due to its higher moisture susceptibility; however, this is also due to the potential simplified reaction occurring in the environment of the road (where the exhaust gases containing CO_2 are present in abundance):

$CaCl_2 + CO_2 + H_2O \rightarrow CaCO_3 + 2\ HCl$

Calcium carbonate, one of the products of the reaction, is insoluble salt which precipitates as a solution concentrate, allowing gaseous hydrochloric acid (strong corrosive agent) to interact with the environment (cars).

A similar simplified reaction can occur with sodium chloride:

$2NaCl + CO_2 + H_2O <-> Na_2CO_3 + 2HCl$

However, because sodium carbonate is a soluble salt, hydrochloric acid is not as readily available for corrosive action in this case.

On the basis of the above, we decided to investigate the behavior of aggregates in salt solutions and in salt solutions acidified (simulating the situation in which part of the carbonates were removed from the original deicing liquid).

7.3 Samples and methodology of reaction experiment

A set of four reactions was conducted in order to establish the reactivity of abraded fines (SRK-test) with deicing chemicals. In place of substrates, we chose fines passing 0.063 mm sieve of the dust from abrasion of Sample 5 B and Reference 1 B, (Table 2, Chapter 3.3). In place of de-icing chemicals, we selected solutions of 20 %wt. of calcium chloride and 20 % wt. sodium chloride. The reaction specific amounts are provided in Table 10. As discussed in the SRK abrasion analysis, a very small amount of fines was available from the Reference 1 sample.

Table 10. *Reaction substrates and their amounts.*

Experiment	Sample 5 OKTO-asphalt dust	Reference 1 normal asphalt dust	20 % wt. $CaCl_2$	20 % wt. NaCl
Reaction 1	4,0 g	-	40,7 g	-
Reaction 2	4,0 g	-	-	40,7 g
Reaction 3	-	1,8 g	40,0 g	-
Reaction 4	-	1,3 g	-	40,0 g

We have used the apparatus presented in Figure 13 to conduct the reaction. Substrates were placed into the round bottom glass flask of 250 ml, capable of rotation and immersed in the water bath. The cooler system was used to prevent extensive evaporation of liquids. Each reaction was conducted at 110 °C, with a rotation frequency of 35 rpm, at 100.4 kPa for a period of 60 minutes. No water condensation was observed below the cooler.

Figure 13. *The apparatus used for the execution of reactions of abraded fines (SRK-test) with deicing solutions.*

After termination of the reaction, 15 ml of ROW was used to wash the round bottom bottle during the transfer of reaction products into the beaker for cool down.

After the sample had cooled down, a separation procedure was implemented. The transfer of the reaction product from beaker to centrifuge tubes required another addition of 15 ml ROW. The centrifuge was set at 1500 rpm for 6 minutes and the supernatant called "first wash" collected. A portion of 20 ml of ROW was used to clean the powder and a second stage of separation was executed. Then the centrifuge was again set at 1500 rpm for 6 minutes and the supernatant called "second wash" collected. A portion of 20 ml of ROW was used to clean the powder and a second stage of separation carried out. The centrifuge was set at 1500 rpm for 6 minutes and the supernatant was discarded. The solid was dried in the oven at 110 °C. The liquid material collected during the purification was partially saved as is and partially evaporated (kept in the form of a powder).

7.4 Samples and methodology of the corrosion resistance experiment

Six aggregates were used for the purpose of investigating the behavior of aggregates typical of the Oulu region in comparison to aggregates and other materials typically used, for example, in the metropolitan area of Helsinki. In the experiment, only fines passing 0.063 mm were used to facilitate similar reactivity. We have chosen two materials characteristic of the Oulu region, namely the man-made OKTO-aggregate and the Huttukylä aggregate, and compared them to the behavior of the Koskenkylä and Teisko aggregate, as well as with the behavior of typically used asphalt concrete fillers – limestone and fly ash.

As it was desired that the reaction occur at normal temperatures, a low concentration of de-icing chemicals was used, because the lower the concentration, the higher the kinetic of the corrosion process. Three experiments were conducted, A, B and C. In the first set-up, six vials were filled with a small amount of fines and covered with 3 ml of the solution of the sodium chloride solution. Due to our prior experience, we expected a reaction to occur spontaneously, however, after a period of 48 hours nothing had occurred. The conditions and observations from the first Experiment A, first reaction (Reaction 1), are presented in Table 11 and Figure 14.

As discussed earlier, the corrosive action of deicing chemicals is assigned to free hydrochloric acid. Thus, in the second Experiment B, (Reaction 2) we decided to use 3 ml of sodium chloride and 0.5 ml of concentrated hydrochloric acid, Table 12 and Figure 15. The third Experiment C used 3.3 ml of 2.2% wt. $CaCl_2$ and 0.5 ml of concentrated hydrochloric acid as supernatant over the fines as seen in Table 13 and Figure 16. In those scenarios, there are about 60 and 120 times more mol of hydrochloric acid than those of sodium chloride and calcium chloride, respectively. It is important to note that this is a rather extreme situation engineered to demonstrate the potential reactivity of the aggregates and not the actual one.

Table 11. Conditions and observations (after 48 h) of Experiment A, Reaction 1.

Vial number	Type of aggregate	Amount	Solution	Observation
1	Teisko	0.1207 g	2.2 %wt. NaCl/3ml	Nothing
2	Fly Ash	0.1180 g	2.2 %wt. NaCl/3ml	Nothing
3	OKTO-aggregate	0.1314 g	2.2 %wt. NaCl/3ml	Not all of OKTO-aggregate dissolves in water-based solution (something organic?)
4	Limestone	0.1361 g	2.2 %wt. NaCl/3ml	Nothing
5	Koskenkylä	0.1552 g	2.2 %wt. NaCl/3ml	Nothing
6	Huttukylä	0.1427 g	2.2 %wt. NaCl/3ml	Nothing, after two days a red color (like rust) observed on the surface of the fines

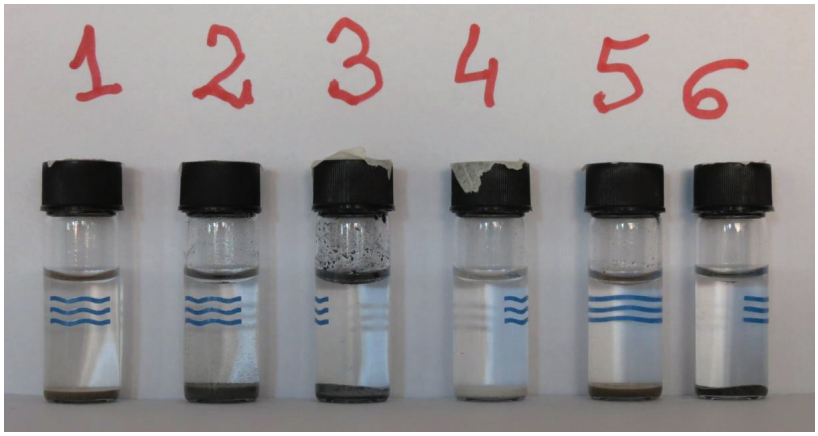

Figure 14. Observation of vials from Experiment A after 48 h.

Table 12. The conditions and observations (immediately after immersion) of Experiment B, Reaction 2.

Vial number	Type of aggregate	Solution	Observation t_0
1	Teisko	2.2 %wt. NaCl/3ml + 0.5 ml conc. HCl_{aq}	Slow bubbling
2	Fly Ash	2.2 %wt. NaCl/3ml + 0.5 ml conc. HCl_{aq}	Green turning yellow stripe above aggregate, bubbling
3	OKTO crushed	2.2 %wt. NaCl/3ml + 0.5 ml conc. HCl_{aq}	Slow bubbling
4	Limestone	2.2 %wt. NaCl/3ml + 0.5 ml conc. HCl_{aq}	Strong bubbling, caused foam which led to over boil
5	Koskenkylä	2.2 %wt. NaCl/3ml + 0.5 ml conc. HCl_{aq}	Very slow bubbling
6	Huttukylä	2.2 %wt. NaCl/3ml + 0.5 ml conc. HCl_{aq}	Small amount of bubbling and yellow stripe forming above aggregate

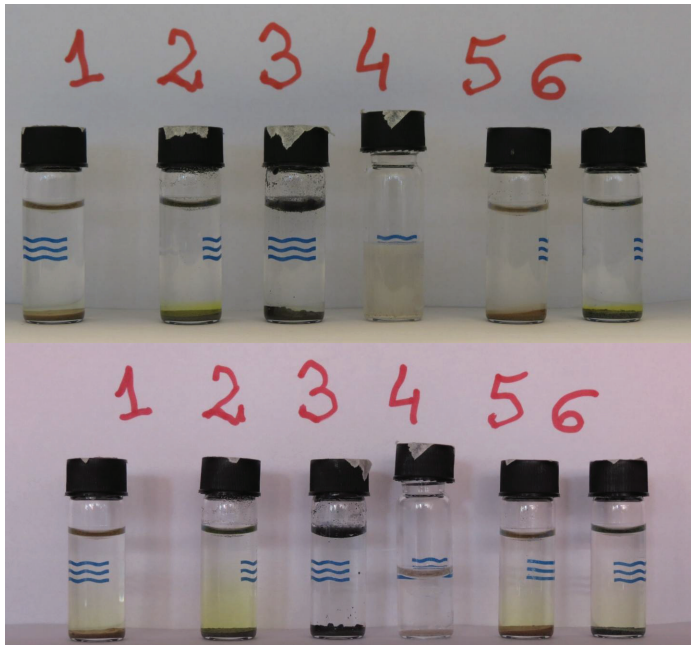

Figure 15. The observations of Experiment B soon after immersion in solution (upper) and 24 h afterwards (lower).

Table 13. The conditions and observations (soon after addition of solution) in Experiment C.

Vial number	Mass of fines (g)	Type of aggregate	Solution	Observation t_0
1	0.1475	Teisko	2.2 %wt. $CaCl_2$/3ml + 0.5 ml conc. HCl_{aq}	Slow bubbling, yellow color coming above the precipitate
2	0.1580	Fly Ash	2.2 %wt. $CaCl_2$/3ml + 0.5 ml conc. HCl_{aq}	Green turning yellow stripe above aggregate, bubbling
3	0.1519	OKTO aggretate	2.2 %wt. $CaCl_2$/3ml + 0.5 ml conc. HCl_{aq}	Vigorous bubbling
4	0.1559	Limestone	2.2 %wt. $CaCl_2$/3ml + 0.5 ml conc. HCl_{aq}	Strong bubbling, stopped after 15 minutes.
5	0.1601	Koskenkylä	2.2 %wt. $CaCl_2$/3ml + 0.5 ml conc. HCl_{aq}	Very slow bubbling
6	0.1540	Huttukylä	2.2 %wt. $CaCl_2$/3ml + 0.5 ml conc. HCl_{aq}	Bubbling, color of the solution faint green.

7.5 Salt reactions results

The reactivity of abraded fines with salt was not evaluated closely as described above. The hypothesis of galvanic series type ion exchange was abandoned upon evaluation of the data coming from the analysis of the car dust. However, no visible coloring of the liquids was observed, leading us to believe that the iron (III) chloride observed in the dust was unlikely to have come from the abraded dust.

In order to demonstrate the low reactivity of the fines, we completed the second experiment (corrosion resistance experiment). It was hypothesized that due to high iron content in the aggregates, the formation of iron chloride could be more pronounced for the OKTO-aggregate. The observations of iron chloride formation reveal that the OKTO-aggregate is unlikely to corrode forming that compound with both $CaCl_2$ and NaCl (see Figure 16 and Figure 15, respectively). The other Oulu region-specific aggregate tested (Huttukylä) revealed some reactivity in NaCl and was very mild (almost invisible) with $CaCl_2$. This remains opposite to the behavior of typical aggregates used in southern Finland, which all expressed a visible susceptibility to corrosion in this type of reaction. As a reminder, this was a demonstrative experiment with the environment of the reaction engineered to pronouncedly corrode the aggregates. In normal circumstances, this action would be much slower and even less visible. As presented in Figure 14, submerging fines for a period of 48 h in sodium chloride solution without shifting the balance to the hydrochloric acid rich situation resulted in no corrosion of aggregates.

On the basis of the results from this experiment, we can conclude that the OKTO-aggregate is not contributing extra iron (III) chloride into the system, thus, a plausible explanation of the pronounced corrosion of car parts is simply their susceptibility to corrosion.

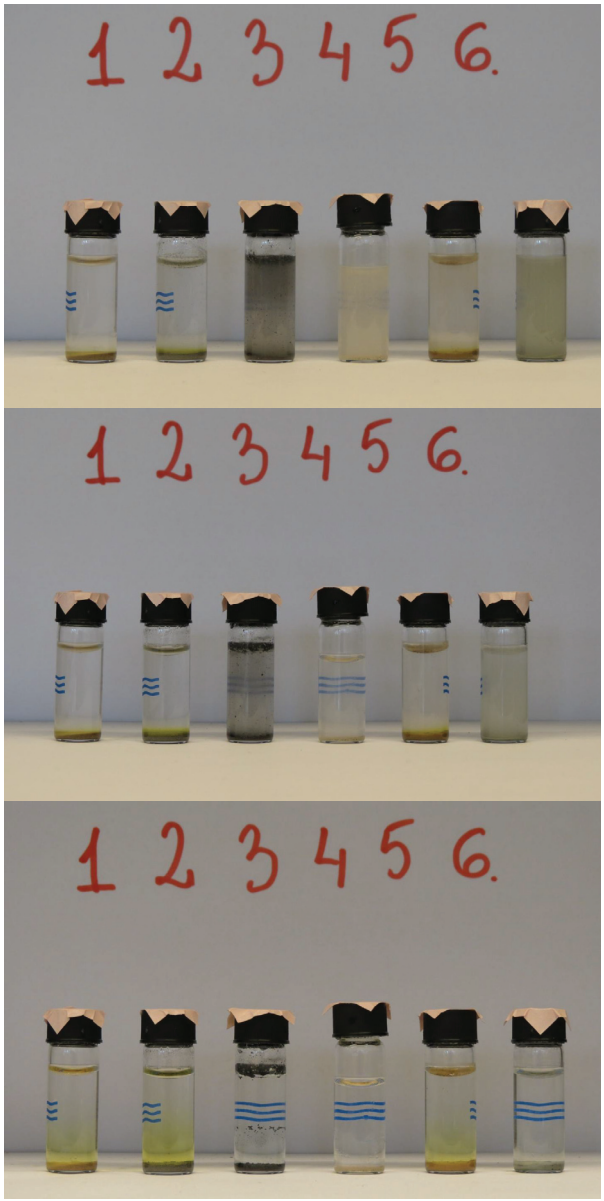

Figure 16 *The observations of Experiment C soon after the addition of solution (upper), 15 minutes (middle) and 24 hours after (lower).*

8 CONCLUSIONS

This research has been initiated as a response of the Finnish Transport Agency to the news published in 2013 linking the man-made OKTO-aggregate to the dust found from car parts in the Oulu region. This dust has been reported to cause damage to the timing belts of cars.

To obtain asphalt dust for analysis, a laboratory test set-up was designed to simulate the studded tire abrasion of asphalt road pavement. With the help of the SRK-device, asphalt mixtures used in the Oulu region were abraded to collect dust for the component analysis. In addition, the OKTO-aggregate and natural aggregates from the Oulu region and other parts of country were investigated.

Using a Field Emission Scanning Electron Microscope and specific commercial software for particle analysis FE-SEM, the Finnish Geoscientific Laboratory studied the mineralogy, composition and size distribution of the dust obtained by SRK-device, four samples of dust from the damaged cars, and OKTO-aggregate. In addition, the composition of the OKTO-aggregate material and the abraded dust obtained by the SRK device was verified and compared by using XRF analysis and Fourier transmission infrared spectrometry (FT-IR).

OKTO-aggregate is the brand name corresponding to the smelter slag of the Outokumpu Company, Tornio ferrochromium plant. The slag material has a slightly porous to massive texture which is similar to some basaltic volcanic rocks which can comprise good to excellent aggregate material for road construction. The hardness of the glassy slag matrix is around 7 in Mosh harness scale. The matrix also includes spinel group minerals as phenocrysts, which characteristically have a hardness ranging from 7 to 8. Therefore, as expected, the abrasion resistance of the OKTO-aggregate asphalt mixture applied in the Oulu region was found to be excellent in the standard Prall-test which measures the impact of studded tires. Both the results of the SRK-dust analysis by FT-IR spectrometry and the particle analysis with FE-SEM suggested that most particles detached from the asphalt mixture represented the rock aggregate used.

Four samples of dust from damaged cars were provided by the Lapland School of Applied Sciences for blind testing. The dust samples were automatically classified into features with distinctive back scattering electrons BSE and or energy dispersive spectrometry EDS-characteristics. The number of particular features classified in each of the four dust samples ranged from 4851-5428. In three samples, the apparently overwhelming proportion of the fragments were iron oxides (Fe_2O_3 FeOOH or Fe_3O_4) comprising 4124-4421 features that represented 72-87 % of the total measured area of the features. The next prominent group of fragments was the common rock forming minerals comprising about 13-27 % of analyzed fragment area. One of the samples contained 4240 mineral fragments and 798 iron oxide fragments that comprised 85 and 12 % of the total area of classified particles, respectively. The number of OKTO features ranged 7-24 representing 0.07-1 % of the total area of classified features. This means that samples have 25 to 1200 mineral fragments for each OKTO fragment. The samples derived from damaged car parts also contained corundum. The number of corundum particles ranged from 4 to 383 or 0.004-0.1 % of the total classified particle area. However, corundum was not found in the OKTO-aggregate specimens obtained with the help of the SRK-device.

The EDS-point analysis results of the car dust samples also reported significant amounts of chloride which suggest that the damage of the timing belts is linked to the use of deicing chemicals. Chloride concentrations do not correlate with sodium or calcium concentrations,

but are associated with high iron concentrations suggesting that chloride was in the form of iron (III) trichloride. The obvious source of iron was iron oxide particles which are a likely result of abrasion and corrosion of the metal parts in the engines. However, the reactions of deicing agents and aggregates could not be excluded as a source of iron. Based on prior research on the effects of deicing chemicals, it was considered plausible that their use, particularly the use of Ca-chlorite, could lead to the precipitation of Fe-chloride in acidic conditions. Therefore, the reactivity of aggregate and filler materials was tested in the laboratory with Na- and Ca chloride solutions and corresponding acidified solutions. The aggregates tested included the OKTO-aggregate, Huttukylä rock aggregate from the Oulu region, Teisko and Koskenkylä rock aggregates used extensively in Southern Finland, as well as fly ash and crushed limestone used as fillers. The other natural rock aggregates revealed themselves to be reactive and precipitating iron chloride. However, the OKTO-aggregate did not produce distinguishable Fe chloride precipitate.

Therefore, the possible contribution of the OKTO-aggregate to the mechanical breakage or abrasion of car parts was considered insignificant compared with the other fragments, such as corundum, that were also detected in the car dust. Moreover, the OKTO-aggregate was found to be much less reactive with deicing chemicals than the rock aggregate used in the Oulu region. To sum up, the OKTO-aggregate does not significantly contribute to the chemical corrosion of car parts.

REFERENCES

Akyuz, S., Akyuz, T., Emre, G., Gulec, A., Basaran, S. Pigment analyses of a portrait and paint box of Turkish artist Feyhaman Duran (1886–1970): The EDXRF, FT-IR and micro Raman spectroscopic studies, Spectrochimica Acta Part A: Molecular and Biomolecular Spectroscopy, Volume 89, April 2012, Pages 74–81.

Cai Y., Hu Y., Song L., Xuan S., Zhang Y., Chen Z., Fan W., Catalyzing carbonization function of ferric chloride based on acrylonitrile-butadiene-styrene copolymer/organophilic montmorillonite nanocomposites, Polymer Degradation and Stability 92 (2007), pp. 490-496.

Dore, G., Zubeck, H., Cold Regions Pavement Engineering ASCE Press, 2009.

Finnish Asphalt Specifications 2000, Finnish Pavement Technology Advisory Council (PANK), Edita Ltd, Helsinki, 2000, ISBN 951-97197-6-8

Finnish Asphalt Specifications 2011. Finnish Pavement Technology Advisory Council, (PANK), Edita Ltd, Helsinki, 2011, ISBN 978-952-99985-0-0.

Gy. P. Sampling of discrete materials - a new introduction to the theory of sampling. Chemo metrics and Intelligent Laboratory systems, Volume 74, 2004, pp 7-24.

Jokinen, H. Ferrokromikuonatuotteiden valmistus, käyttö ja ympäristökelpoisuus, Avesta Polarit Stainless, Tornio research centre, Report no. 5397-5380/2002.

Ma C., Beckett J.R. and Rossman G.R. Discovery of a new chromium sulfide mineral, Cr5S6, in Murchison. 73rd Annual Meteoritical Society Meeting, 2010. Available in http://www.lpi.usra.edu/meetings/metsoc2010/pdf/5135.pdf (site visited 15.8.2014).

Makowska, M., Pellinen, T., Olmos Martinez, P., Laukkanen, O.-V. *Analytical methodology to determine the composition of filler used in HMA*: Case study, Transportation Research Record: Journal of the Transportation Research Board, Issue Number: 2445, Publisher: Transportation Research Board, ISSN: 0361-1981, 2014, pp 12–20.

Nevalainen, N. The use of thermal camera for quality assurance of asphalt pavement construction, Master's thesis, Aalto University, 2014.

Outokumpu Oyj, Material Safety Data Sheet: OKTO-murske (OKTO-aggregate). 6.08.2013.

Työterveyslaitos/International Programme on Chemical Safety (IPCS). Rautakloridi, kemikaalikortti, http://kappa.ttl.fi/kemikaalikortit/khtml/nfin1499.htm accessed at 9.6.2014.

Reimer L. Scanning electron Microscopy Physics of Image Formation and Microanalysis. 2nd ed. Heidelberg, Germany: Springer. 527 p. Springer Series in Optical Sciences Volume 45, 1998. ISBN 3-540-63976-4.

Sassi, J. Tutkimus autojen hammashihnavälitteisen jakopään kestävyysongelmista. Lapin Ammattikorkeakoulu, Kone- ja tuotantotekniikan opinnäytetyö, Kemi 2014, p. 44.

Vahur, S., Teearu, A., Leito, I. ATR-FT-IR spectroscopy in the region of 550–230 cm−1 for identification of inorganic pigments, Spectrochimica Acta Part A: Molecular and Biomolecular Spectroscopy, Volume 75, Issue 3, March 2010, Pages 1061–1072.

Vaughan D.J. and Wogelius R.A. (eds.) Environmental Mineralogy. Budapest, Hungary. Eötvös University Press. 434 s. European Mineralogical Union Notes in Mineralogy Volume 2, 2000. ISBN 963-463-133-9.

Vestola, E., Pohjanne, P., Carpén, L., Kaunisto, T., Ahlroos, T. Kalsiumkloridin sivuvaikutukset, Tiehallinnon selvityksiä 38/2006, Tiehallinto, Helsinki 2006.

Appendix A: Diffractogram of OKTO-aggregate

Analysis carried out by Juha Larismaa, Aalto School of Chemistry, Department of Material Sciences.

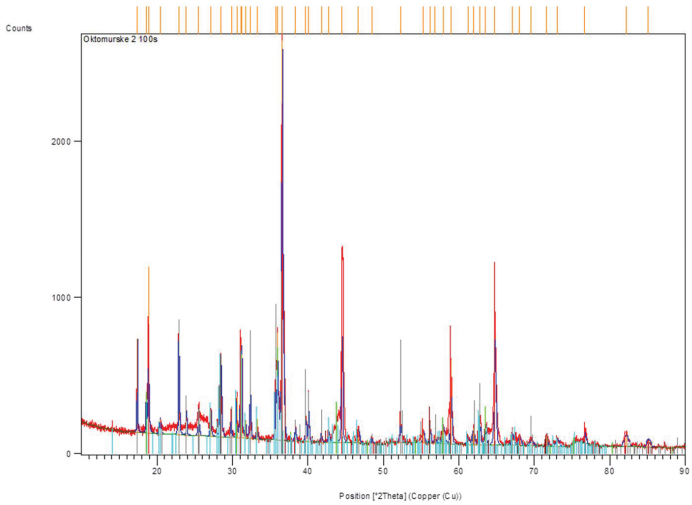

Appendix B. SEM-EDS analysis

Energy dispersive spectrometry analysis of dust samples obtained by SRK-abrasion tests (Clean 31.1.14-C and Clean 5.2.14-C) and three dust samples (Dust 2-4) from damaged cars using field emission scanning electron microscope in GTK. Each point represents composition in an area with about 10µm diameter. These analyses were done to support automatic particle detection by providing information on the different phases in the samples.

Sample: Clean 31.1.14 C
Type: C-coated
LV SEM
Processing option : All elements analysed (Normalised)

All results in weight%

Spectrum	O	Na	Mg	Al	Si	S	Cl	K	Ca	Ti	Cr	Mn	Fe	Ni	Cu	Zn	Ta	W	Total	Comment
Spectrum 4			0,00	0,00	0,45	2,74					3,04		93,77						100,00	ruostumaton teräs
Spectrum 3				0,00	0,00	1,25					3,27		94,52	0,95					100,00	ruostumaton teräs
Spectrum 3				0,59	0,92						3,93		94,56						100,00	ruostumaton teräs
Spectrum 1				0,53	0,38						3,11		94,33		1,64				100,00	ruostumaton teräs
Spectrum 2	41,31		2,86	1,73	3,83		0,41		0,81	21,25	0,75	0,97	26,07						100,00	ilmeniitti
Spectrum 20	29,19		0,47	0,53	1,14				0,55	17,67	0,66	1,09	46,00		1,10	1,59			100,00	ilmeniitti + Fe ox
Spectrum 16	27,30		13,89	11,09	0,43						43,63		3,66						100,00	kromiitti
Spectrum 16	37,98		10,52	12,16	0,00						33,22		6,12						100,00	kromiitti
Spectrum 9	35,54		9,08	8,04	1,61				0,25	0,37	33,04		12,06						100,00	kromiitti
Spectrum 5	38,93		10,47	11,33	1,77				0,39	0,42	31,17		5,53						100,00	kromiitti
Spectrum 14	31,81		8,72	8,74	4,34		0,51		1,30		30,60		13,97						100,00	kromiitti
Spectrum 17	34,50		9,58	8,63	3,16				0,63		29,68		13,82						100,00	kromiitti
Spectrum 18	39,23		13,32	14,82	0,67						29,32		2,64						100,00	kromiitti
Spectrum 19	40,48		13,98	16,64	1,30				0,27		26,25		1,07						100,00	kromiitti
Spectrum 4	41,36		14,67	23,24	0,43						19,36		0,94						100,00	Cr-spinelli
Spectrum 13	41,99		15,71	27,77	0,81						12,94		0,78						100,00	Cr-spinelli
Spectrum 15	42,10		15,36	29,20	0,00						12,53		0,81						100,00	Cr-spinelli
Spectrum 7	42,52		15,43	28,62	0,00				0,27		12,19		0,97						100,00	Cr-spinelli

Spectrum 17	42,69		13,69	24,86	6,19			0,39	0,24	11,01		0,92					100,00	Cr-spinelli
Spectrum 20	22,05		3,54	5,21	0,00			1,02	0,99	1,50		1,51	0,88		9,91	53,39	100,00	Ta-W-yhdiste?
Spectrum 7	23,00		4,93	4,31	15,46	0,51	0,41	4,33		8,58	0,78	32,61		5,08			100,00	sekaspektri?
Spectrum 13	47,68	0,60	4,82	11,97	26,02	0,78	0,29	3,78	0,49	3,06		0,52					100,00	sekaspektri? kloriitti + hbl
Spectrum 12	45,60		17,93	8,97	24,31				0,67	2,51		0,00					100,00	Cr-pitoinen kloriitti
Spectrum 6	46,45		19,18	5,67	24,94				0,70	2,40		0,65					100,00	Cr-pitoinen kloriitti
Spectrum 12	33,78		10,23	12,13	34,70		0,75	3,51	1,00	2,40	0,49	1,00					100,00	Cr-pitoinen kloriitti
Spectrum 1	42,91		11,77	10,39	29,81			2,07	0,67	1,89		0,48					100,00	Cr-pitoinen kloriitti
Spectrum 15	39,31		9,96	11,36	33,18		0,48	2,94	0,50	1,81		0,47					100,00	Cr-pitoinen kloriitti
Spectrum 19	46,64	0,48	4,84	11,77	28,19	0,35	0,82	4,19	0,53	1,66		0,52					100,00	Kloriittiutunut sarviv.
Spectrum 10	47,80		4,29	11,00	29,99		0,45	2,99	0,85	1,58	0,41	0,64					100,00	Kloriittiutunut sarviv.
Spectrum 8	43,73	0,70	5,96	7,05	21,81			8,07		0,42		12,25					100,00	sarvivälke
Spectrum 10	48,38		10,23	10,89	14,37				0,25	0,40		15,48					100,00	Cr-pitoinen kloriitti
Spectrum 14	42,91		9,23	1,89	27,17			8,92		0,34		9,55					100,00	sarvivälke
Spectrum 11	47,48		9,08	3,03	23,54			7,29		0,33		9,25					100,00	sarvivälke
Spectrum 2	45,67			14,38	18,44			16,87		0,00		4,63					100,00	zoisiitti
Spectrum 18	45,77			14,42	18,63			16,69		0,00		4,49					100,00	zoisiitti
Spectrum 6	49,24	0,72	4,82	7,57	19,42			7,16	0,28	0,00		10,79					100,00	sarvivälke
Spectrum 11	46,50	0,84	5,14	7,70	20,45		0,29	7,59	0,24	0,00		11,24					100,00	sarvivälke
Spectrum 9	44,57		9,09	0,94	26,38			9,11		0,00		9,91					100,00	sarvivälke
Spectrum 8	49,03	5,14	0,00	12,76	28,00			5,07		0,00		0,00					100,00	albiitti
Spectrum 5	49,01	5,64	0,00	12,03	30,17		0,40	2,74		0,00		0,00					100,00	albiitti

Clean 5.2.14 C

Spectrum	O	Na	Mg	Al	Si	S	Cl	K	Ca	Ti	Cr	Mn	Fe	Ni	Cu	Zn	Ta	W	Total	Comment
Spectrum 14	37,33		13,17	10,84						0,37	37,05		1,23						100	kromiitti
Spectrum 16	37,44		12,81	7,98	0,72				0,36		34,32		6,37						100	kromiitti
Spectrum 22	36,53		11,45	8,12	0,42						34,30		9,19						100	kromiitti
Spectrum 18	28,04		9,07	8,34	1,81				0,52	0,40	27,01		24,81						100	kromiitti
Spectrum 11	37,20		12,97	15,66						0,30	26,49		7,38						100	kromiitti
Spectrum 25	22,62		5,33	7,59	21,08			0,63	1,75		20,84		20,16						100	kromiitti
Spectrum 20	39,52		13,63	23,64	2,67				1,56		16,50		2,47						100	Cr-spinelli
Spectrum 1	43,02		15,25	27,00							14,01		0,72						100	Cr-spinelli
Spectrum 18	45,29		11,29	18,12	8,97		0,58		3,50		7,55		4,71						100	Cr-spinelli +
Spectrum 2						0,71					2,71		96,58						100	ruostumaton teräs
Spectrum 4			0,95	0,95	1,65				0,35		0,62		95,48						100	ruostumaton teräs
Spectrum 1			0,84	2,23	1,11				0,34		2,95		92,53						100	ruostumaton teräs
Spectrum 6	13,83		2,74	2,78	5,83				0,62		0,60		72,84	0,76					100	ruostumaton teräs
Spectrum 8	13,32		2,23	3,45	3,35	3,07	0,40		0,73		3,66		65,88		1,62	2,31			100	ruostumaton teräs
Spectrum 3			1,05	0,68	0,81	38,71			0,45		1,86		55,52	0,93					100	Pyrrhot.
Spectrum 23	47,02		4,84	20,21	18,05				4,89				4,99						100	Mg Fe Ca Al-silik
Spectrum 15	48,54	3,57		14,47	25,81				7,61										100	Plag.
Spectrum 7	30,32		11,17	1,07	33,86				11,40		0,48		11,71						100	sarvivälke
Spectrum 17	33,57		9,18	2,13	30,71				11,31				13,11						100	sarvivälke
Spectrum 5	39,62		6,82	5,51	24,72				10,31				13,02						100	sarvivälke
Spectrum 12	36,89		9,27	2,61	30,20				10,17				10,85						100	sarvivälke
Spectrum 16	40,15		5,77	6,26	25,05				9,00	0,37			13,39						100	sarvivälke
Spectrum 21	41,75		7,05	5,60	24,85				8,91				11,84						100	sarvivälke
Spectrum 8	42,09	0,59	4,59	7,95	22,11			0,41	8,73			0,47	13,07						100	sarvivälke
Spectrum 9	43,99		6,14	5,95	22,88				8,68				12,36						100	sarvivälke
Spectrum 15	45,86		8,10	2,04	25,41				8,37				10,22						100	sarvivälke
Spectrum 3	45,00	0,64	5,23	6,75	21,05			0,32	8,34	0,27			12,41						100	sarvivälke
Spectrum 21	43,73		8,53	0,89	27,03				8,31			0,41	11,10						100	sarvivälke
Spectrum 24	43,61	0,73	4,47	8,16	22,14				8,22				12,68						100	sarvivälke
Spectrum 9	46,82		8,95	1,04	26,09				8,14				8,95						100	sarvivälke
Spectrum 6	44,92	0,66	4,20	7,90	21,09			0,36	8,05				12,82						100	sarvivälke
Spectrum 2	44,72	0,76	6,66	5,85	22,49				7,93			0,37	11,23						100	sarvivälke

Spectrum 12	44,65	0,83	5,03	7,64	21,60		0,38	7,77			12,11			100	sarvivälke
Spectrum 20	45,52		7,81	4,37	23,93			7,57		0,37	10,43			100	sarvivälke
Spectrum 7	46,72	0,89	5,19	6,98	22,93			7,48			9,81			100	sarvivälke
Spectrum 4	49,46		8,73	1,71	24,84			7,32			7,94			100	sarvivälke
Spectrum 13	46,45	0,49	3,98	11,30	30,16		0,74	6,09		0,81				100	sarvivälke
Spectrum 17	49,51	0,63	4,31	8,88	26,34		0,33	5,18	0,52	0,63	3,67			100	sarvivälke
Spectrum 10	47,95	0,34	4,67	11,00	27,80	0,29	0,52	4,81	0,43	1,25	0,41	0,52		100	Cr-pitoinen kloriitti
Spectrum 22	47,22	0,31	6,60	10,80	28,67		0,85	3,47	0,59	1,15	0,34			100	Cr-pitoinen kloriitti
Spectrum 10	48,89		4,98	9,96	28,37	0,47		3,42	1,91	0,40		1,60		100	Cr-pitoinen kloriitti
Spectrum 13	48,86		5,26	11,07	30,39		0,25	2,29		1,89				100	Cr-pitoinen kloriitti
Spectrum 11	41,05		7,05	9,99	27,86		0,51	2,00	0,41	3,40		7,74		100	Cr-pitoinen kloriitti
Spectrum 5	43,08		24,77	4,56	22,74	0,60		1,05		2,32			0,88	100	Cr-pitoinen kloriitti
Spectrum 19	47,50		18,15	6,53	24,07			0,41	0,59	2,12		0,63		100	Cr-pitoinen kloriitti
Spectrum 19	54,20		0,63	0,31	0,66			44,20						100	Kalsiitti
Spectrum 14	56,04							43,96						100	Kalsiitti

Sample: DUST 2

LV SEM

Processing option : All elements analysed (Normalised)

All results in weight%

Spectrum	O	Na	Mg	Al	Si	P	S	Cl	K	Ca	Ti	Cr	Mn	Fe	Co	Cu	Zn	Total	
Spectrum 5	20,47				0,66			0,46						78,40				100,00	Fe ox
Spectrum 20	18,17							6,04						75,79				100,00	Fe ox + suola
Spectrum 1	20,66				0,59			0,57						75,21		1,07	1,90	100,00	Fe ox + suola Zn
Spectrum 11	20,44				1,39			0,86		0,41				74,17		2,72		100,00	Fe ox + suola
Spectrum 54	23,53				0,73			0,59						74,00		1,15		100,00	Fe ox + suola
Spectrum 14	21,79				1,09			0,92						73,91			2,29	100,00	Fe ox + suola Zn
Spectrum 18	22,63				1,52			1,13		0,87				73,85				100,00	Fe ox + suola
Spectrum 23	23,86				0,77			0,58		1,25				73,55				100,00	Fe ox + suola
Spectrum 38	23,48				0,81					1,00				73,45			1,26	100,00	Fe + messinki
Spectrum 15	23,71				2,45			0,86						72,97				100,00	Fe ox + suola
Spectrum 48	25,55				0,92			0,94						72,60				100,00	Fe ox + suola
Spectrum 36	23,80				2,00			1,08		0,88				72,23				100,00	Fe ox + suola
Spectrum 25	26,04				0,74			1,10						72,13				100,00	Fe ox + suola
Spectrum 37	26,04							2,21						71,76				100,00	Fe ox + suola
Spectrum 8	24,10				0,66			0,44		0,41				71,56		1,44	1,38	100,00	Fe ox + suola Zn
Spectrum 9	24,32				1,04					1,13				71,56			1,95	100,00	Fe ox + suola Zn
Spectrum 44	15,49			1,05	3,75	0,92	1,07			0,96			1,18	70,03		1,37	4,18	100,00	Fe ox + messinki?
Spectrum 30	26,91				1,54									68,98		1,23	1,35	100,00	Fe ox + messinki?
Spectrum 26	22,85				1,64		0,49	0,66		0,64			0,86	68,88		1,28	2,69	100,00	Fe ox + suola Zn
Spectrum 45	27,07				2,36			0,92		1,27				68,38				100,00	Fe ox + epoxi (Cl)
Spectrum 40	26,96	0,00			2,48			0,54		0,47				67,77			1,78	100,00	Fe ox + suola Zn
Spectrum 3	28,48				3,11			0,57						67,09	0,75			100,00	Fe ox + suola
Spectrum 10	24,61	0,00		0,71	2,41			0,58	0,43	0,58				66,89		1,64	2,15	100,00	Fe ox + suola Zn
Spectrum 35	29,52				1,14			0,96						66,68			1,69	100,00	Fe ox + suola Zn
Spectrum 4	29,00				1,59			3,76						65,65				100,00	Fe ox + suola
Spectrum 39	25,67			1,22	5,27			1,41		1,13				65,29				100,00	Fe ox + suola
Spectrum 12	21,32			2,80	8,07			1,35		2,13				64,33				100,00	Fe ox + suola

Spectrum 16	33,62						2,48		0,83			63,07		100,00	Fe ox + suola
Spectrum 46	32,00				6,58		1,80		0,82			58,80		100,00	Fe ox + suola
Spectrum 27	34,18				4,87		2,10					56,85	2,01	100,00	Fe ox + suola Zn
Spectrum 52	43,38						5,27					51,35		100,00	Fe ox + suola
Spectrum 51	40,68			2,91	2,04		4,32					50,06		100,00	Fe ox + suola
Spectrum 31	47,92						3,19					48,89		100,00	Fe ox + suola
Spectrum 50	39,32		5,32		0,92		0,89		8,42	0,56		42,94	1,64	100,00	Fe ox + suola Zn
Spectrum 34	34,09					29,37	2,22					34,32		100,00	Fe ox + suola
Spectrum 13	61,60						7,48					30,92		100,00	Fe ox + suola
Spectrum 53	31,69		9,33		31,49				0,70			26,79		100,00	oliviini
Spectrum 29	67,64						9,71					22,65		100,00	Fe ox + suola
Spectrum 49	38,19		3,04	8,34	21,83			0,60	9,05			18,95	0,00	100,00	Tremol
Spectrum 42	25,58			7,76	33,27		4,74	11,86				16,80		100,00	Biotiitti
Spectrum 41	45,43	3,86		8,61	21,33		3,82		2,04			14,90		100,00	plag + Fe ox
Spectrum 6	43,24	0,86	4,57	7,18	20,96			0,38	8,22			14,58		100,00	plag + Fe ox
Spectrum 43	42,42	0,57	8,03	2,89	24,62			0,39	9,13			11,95		100,00	Tremol
Spectrum 22	46,96	0,72	6,26	5,53	21,89				7,91			10,74		100,00	plag + Fe ox
Spectrum 32	70,57				6,85		10,54	2,67				9,38		100,00	Fe ox + suola
Spectrum 2	45,66	2,71		11,88	23,79				10,18			5,77		100,00	plag + Fe ox
Spectrum 28	21,50		16,12						59,71			2,67		100,00	kalsiitti
Spectrum 21	44,27		8,77	17,17	18,26			0,92	1,55		6,54	2,52		100,00	Cr kloriitti
Spectrum 17	47,50	0,67		18,92	22,81			8,52		0,42		1,16		100,00	Biotiitti
Spectrum 24	45,43		20,21	4,97	26,00					0,45	1,97	0,98		100,00	Cr krysotiili?
Spectrum 47	49,89				49,28							0,83		100,00	Kvartsi
Spectrum 19	46,38	3,80		14,17	27,08				7,76			0,81		100,00	plagioklaasi
Spectrum 33	52,31				47,69									100,00	Kvartsi
Spectrum 7	51,08				48,92									100,00	Kvartsi

Sample: DUST 3

Type: C-coated

ID:

Processing option : All elements analysed (Normalised)

LV SEM

All results in weight%

Spectrum	O	Na	Mg	Al	Si	P	S	Cl	K	Ca	Ti	Cr	Fe	Ni	Cu	Zn	Total	
Spectrum 17						0,53							96,82	2,65			100,00	Teräs
Spectrum 22	8,48					0,74							88,55	2,23			100,00	Teräs
Spectrum 21	10,09				0,56	0,61		0,60					84,75	3,39			100,00	Teräs
Spectrum 8	15,10				0,65	0,63		0,91					81,34	1,37			100,00	Teräs
Spectrum 7	19,40				2,05			0,72					74,48	1,76		1,58	100,00	Teräs + Zn
Spectrum 14	21,47				1,03			0,54					73,19	2,04		1,73	100,00	Teräs + Zn
Spectrum 18	23,13	0,00			1,51			1,08					71,20	1,54		1,53	100,00	Teräs + Zn
Spectrum 19	23,09				1,99			1,07					70,09	2,03		1,75	100,00	Teräs + Zn
Spectrum 13	22,22	1,71			2,93			1,57		0,47			69,54			1,56	100,00	Teräs + Zn
Spectrum 9	28,11												69,50	2,39			100,00	Teräs + Zn
Spectrum 1	27,01				1,99			0,97		0,37			66,68	1,54		1,45	100,00	Teräs + Zn
Spectrum 24	26,42	0,00			2,31	0,57		1,02		0,43			65,96	1,63		1,65	100,00	Teräs + Zn
Spectrum 3	27,92				1,56	0,68		1,17		0,38			65,83	2,45			100,00	Teräs + Zn
Spectrum 20	25,83				2,06			1,25					65,59	2,52	1,18	1,56	100,00	Teräs + Zn
Spectrum 5	24,64				3,56	0,62		0,91		0,51			64,74	2,10	1,10	1,81	100,00	Teräs + Zn
Spectrum 6	29,40	0,00			2,73	0,52		0,92					62,51	1,66		2,25	100,00	Teräs + Zn
Spectrum 11	24,51	1,90		1,28	4,55			1,09		0,63			61,88	1,67		2,49	100,00	Teräs + Zn
Spectrum 16	29,17	0,00		0,77	3,08			1,11		0,38			61,54	1,96		1,99	100,00	Teräs + Zn
Spectrum 10	28,60	0,00		9,63	3,94			0,87					54,54	1,29		1,12	100,00	Teräs + Zn
Spectrum 12	29,37	3,46		2,45	9,31			1,72		1,36			49,79	2,54			100,00	Teräs
Spectrum 23	23,60			2,73	5,84			4,23		1,79			35,61	2,37		23,84	100,00	Teräs + Zn
Spectrum 4	44,18			11,63	18,24					15,80			9,34	0,82			100,00	Epidootti
Spectrum 15	50,07	2,68		9,38	27,85			0,31	7,28	1,06			0,64	0,72			100,00	Muskoviitti
Spectrum 2	47,49		7,63	11,27	25,76		0,23		0,70	3,28	0,54	1,89	0,61	0,61			100,00	Cr kloriitti

Sample: DUST 4
Type: C-coated
ID:
LV SEM
Processing option : All elements analysed (Normalised)

All results in weight%

Spectrum	O	Na	Mg	Al	Si	P	S	Cl	K	Ca	Ti	Fe	Co	Cu	Zn	As	Total	
Spectrum 24					1,03	0,68						98,29					100,00	Valurauta
Spectrum 1						0,95						97,40	1,65				100,00	Valurauta
Spectrum 7	6,00				0,53	0,52		0,36				92,59					100,00	Valurauta+ ox
Spectrum 8	8,10				0,73							91,17					100,00	Valurauta+ ox
Spectrum 22	9,41			0,59	1,49			0,62				87,89					100,00	Valurauta+ ox
Spectrum 15	12,59				1,68			0,54				85,19					100,00	Valurauta+ ox
Spectrum 2	11,61			0,71	1,79			0,51		0,32		85,06					100,00	Valurauta+ ox
Spectrum 4	11,77			0,93	1,44							84,58		1,28			100,00	Valurauta+ ox
Spectrum 20	17,43				1,73			2,03				78,81					100,00	Valurauta+ ox
Spectrum 17	12,19					4,76	4,44	7,34				71,26					100,00	Valurauta+ ox+suola
Spectrum 18	24,57			1,93	3,51			2,22				67,77			0,00		100,00	Valurauta+ ox+suola
Spectrum 14	30,31				0,65			1,42				67,62					100,00	Valurauta+ ox+suola
Spectrum 19	30,98			2,14	5,20			1,46	0,62	0,50		57,92			0,00	1,18	100,00	Valurauta+ ox+suola
Spectrum 16	27,77			3,38	8,75			1,73		1,38	1,21	55,78					100,00	Valurauta+ ox+suola
Spectrum 12	49,79		2,99	4,46	10,26			4,60		1,98		25,92					100,00	Valurauta+ ox+suola
Spectrum 5	41,32		5,10	9,31	18,16				8,36		2,07	15,68					100,00	Biotiitti
Spectrum 11	49,37		4,20	16,51	23,13							6,79					100,00	Kloriitti
Spectrum 21	42,92	4,49		13,74	31,39				0,52	5,94		1,01					100,00	Plag
Spectrum 3	48,12	2,98		14,85	25,32					8,17		0,57					100,00	Plag
Spectrum 10	53,46			0,00	46,05							0,49					100,00	Kvartsi
Spectrum 9	57,66			0,00	41,45			0,46				0,43					100,00	Kvartsi
Spectrum 23	49,70	3,66		9,07	33,27					3,91		0,40					100,00	Plag
Spectrum 13	47,43	6,83		11,52	31,29					2,56		0,36					100,00	Plag
Spectrum 6	48,48	0,83		17,19	21,40					12,09		0,00					100,00	Zoisiitti

This research has been conducted in collaboration with Liikennevirasto (Finnish Transport Agency).

Aalto-ST 1/2015

ISBN 978-952-60-6104-7 (pdf)
ISSN-L 1799-4896
ISSN 1799-4896 (printed)
ISSN 1799-490X (pdf)

Aalto University
School of Engineering
Department of Civil and Environmental Engineering
www.aalto.fi

BUSINESS + ECONOMY

ART + DESIGN + ARCHITECTURE

SCIENCE + TECHNOLOGY

CROSSOVER

DOCTORAL DISSERTATIONS